NAVAL POSTGRADUATE SCHOOL
Monterey, California

THESIS

THE INFLUENCE OF PHYSICAL SYSTEM PARAMETERS ON THE PERFORMANCE OF ADAPTIVE FILTERS FOR SYSTEM IDENTIFICATION OF MECHANICAL SYSTEMS

by

Michael R. Dargel

September, 1996

Thesis Advisor: Robert M. Keolian
Thesis Co-Advisor: Roberto Cristi

Approved for public release; distribution is unlimited.

REPORT DOCUMENTATION PAGE	Form approved OMB No. 0704-188

Public reporting burden for this collection of information is estimated to average 1 hour per response, including the time for reviewing instructions, searching existing data sources, gathering and maintaining the data needed, and completing and reviewing the collection of information. Send comments regarding this burden estimate or any other aspect of this collection of information including suggestions for reducing this burden, to Washington Headquarters services, Directorate for Information Operations and Reports, 1215 Jefferson Davis Highway, Suite 1204, Arlington, VA 22202-4302, and to the Office of Management and Budget, Paperwork Reduction Project (0704-0188), Washington, DC 20503.

1. AGENCY USE ONLY (*Leave Blank*)	2. REPORT DATE	3. REPORT TYPE AND DATES COVERED
	September 1996	Master's Thesis

4. TITLE AND SUBTITLE
THE INFLUENCE OF PHYSICAL SYSTEM PARAMETERS ON THE PERFORMANCE OF ADAPTIVE FILTERS FOR SYSTEM IDENTIFICATION OF MECHANICAL SYSTEMS

5. FUNDING NUMBERS

6. AUTHOR(S)
Dargel, Michael R.

7. PERFORMING ORGANIZATION NAME(S) AND ADDRESS(ES)
Naval Postgraduate School
Monterey, CA 93943-5000

8. PERFORMING ORGANIZATION REPORT NUMBER

9. SPONSORING/MONITORING AGENCY NAME(S) AND ADDRESS(ES)

10. SPONSORING/MONITORING AGENCY REPORT NUMBER

11. SUPPLEMENTARY NOTES
The views expressed in this thesis are those of the author and do not reflect the official policy or position of the Department of Defense or the U.S. Government.

12a. DISTRIBUTION/AVAILABILITY STATEMENT
Approved for public release; distribution is unlimited.

12b. DISTRIBUTION CODE

13. ABSTRACT (Maximum 200 words)

Recursive and nonrecursive least mean square adaptive filters were used to predict the output of various mechanical systems for a given input. The effects of quality factor (Q), dispersion, and transmission time on adaptive filter performance were investigated. Optimal filter delay times and tap weight vector lengths were determined.

14. SUBJECT TERMS
Adaptive Filters, System Identification, Least Mean Square Algorithm

15. NUMBER OF PAGES 86

16. PRICE CODE

17. SECURITY CLASSIFI-CATION OF REPORT	18. SECURITY CLASSIFI-CATION OF THIS PAGE	19. SECURITY CLASSIFI-CATION OF THIS ABSTRACT	20. LIMITATION OF ABSTRACT
Unclassified	Unclassified	Unclassified	UL

NSN 7540-01-280-5500

Standard Form 298 (Rev. 2-89)
Prescribed by ANSI Std 239-18

Approved for public release; distribution is unlimited.

THE INFLUENCE OF PHYSICAL SYSTEM PARAMETERS ON THE PERFORMANCE OF ADAPTIVE FILTERS FOR SYSTEM IDENTIFICATION OF MECHANICAL SYSTEMS

Michael R. Dargel
Lieutenant, United States Navy
B.S.M.E., Norwich University, 1990

Submitted in partial fulfillment of the
requirements for the degree of

MASTER OF SCIENCE IN ENGINEERING ACOUSTICS

from the

NAVAL POSTGRADUATE SCHOOL
September 1996

Author: _____
Michael R. Dargel

Approved by: _____
Robert M. Keolian, Principal Advisor

_____
Roberto Cristi, Co-Advisor

_____
Robert M. Keolian, Chairman,
Engineering Acoustics Academic Committee

ABSTRACT

Recursive and nonrecursive least mean square adaptive filters were used to predict the output of various mechanical systems for a given input. The effects of quality factor (Q), dispersion and transmission time on adaptive filter performance were investigated. Optimal filter delay times and tap weight vector lengths were determined.

TABLE OF CONTENTS

I. INTRODUCTION

This work is a result of investigations into methods of eliminating own ship vibrations from submarine conformal sonar arrays. Future arrays may utilize hydrophones that respond to a sound wave's velocity in place of traditional pressure sensitive hydrophones. In order to detect an incoming signal with such a hydrophone it is necessary to remove signals due to own ship vibrations from the hydrophone's output. Previously this has been accomplished using large metal plates to damp ship vibrations. Because of the high cost and weight of these plates, it is desirable to instead electronically remove own ship vibration signals from the sensor output.

Because of changing machinery lineups, ship speed, depth and other time varying parameters, traditional fixed filters are not adequate to remove own ship vibration signals from the hydrophone output. One method of dealing with systems with time varying characteristics is with adaptive filter algorithms which continuously generate an optimal impulse response describing the physical system. Adaptive filters have been used in acoustic noise cancellation and in system identification for several years [Ref. 1,2].

In this project both recursive (IIR) and nonrecursive (FIR) filters were used to predict the output of the following mechanical systems:

1. Torsion waves in an undamped aluminum rod (a high Q system)
2. Torsion waves in a damped plastic rod (a low Q system)
3. Flexural waves in a damped aluminum rod (a dispersive system)
4. Flexural waves in a damped plastic rod (a dispersive system)
5. Longitudinal waves in a plastic bar (a nondispersive system)
6. Longitudinal waves in a plate (a high Q, multipath system)
7. Longitudinal waves in a metal ring (a high Q, multipath system)

It is hoped that the results of these experiments on the effects of system physical parameters on adaptive filter performance can also be applied to more advanced methods of system identification.

II. BACKGROUND THEORY

A. THE LEAST MEAN SQUARE ALGORITHM

An adaptive filter is a filter that has the property of adjusting its characteristics in response to varying system characteristics. The adaptive filter algorithm generates an impulse response, w(t), describing a system and continuously refines it based on measured system inputs and outputs. Adaptive systems have many applications including prediction, system identification and interference cancellation. In this study adaptive filters utilizing the least mean square algorithm are used to predict the output of simple mechanical systems for a given input signal. A block diagram is shown below:

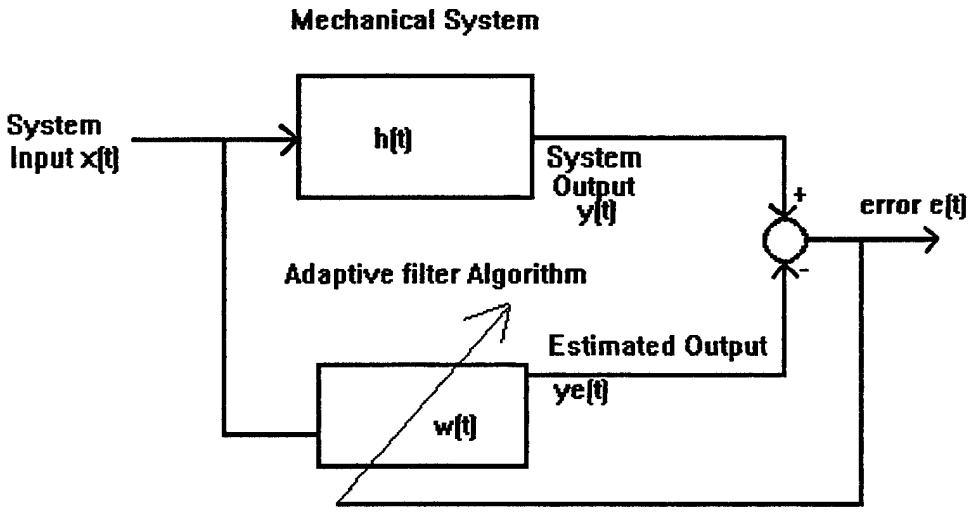

Figure 1 Adaptive System Identification Diagram

The adaptive filter algorithm generates an optimal impulse response to approximate the behavior of a physical system which has an impulse response h(t). In this study the physical system is simply a vibrating piece of plastic or aluminum excited by broadband noise. These systems in general act like low

pass filters in that they attenuate high frequency vibrations more than low frequency vibrations and are thus easily modeled by adaptive filters.

Adaptive filters require a "desired response" in order for the filter to develop this optimal impulse response. In this case, the desired response is the output of the physical system, y(t). The adaptive filter also utilizes an error signal, y(t)-ye(t), where ye(t) is the adaptive filter output. In this system identification application the least mean square algorithm is used to implement the adaptive filter. The following is an outline of how this algorithm is developed [Ref. 3].

The error signal produced in the adaptive algorithm is

$$e(t)=y(t)-ye(t)\,, \tag{1}$$

where y(t) is the output of the physical system and ye(t) is the adaptive filter's estimate of that output. The estimated output, ye(t), is determined by multiplying the input x(t) by the estimated impulse response w(t). The vector w(t) is initially all zeros but is developed into an estimate of the actual impulse response h(t) by the adaptive filter algorithm. Using the tap weight vector of the adaptive filter, w(t), in Eq. 1 results in:

$$e(t)= y(t)-x(t)^t w(t\,)=y(t)-w^t(t)x(t). \tag{2}$$

Dropping the time dependence for clarity, the error squared is:

$$e^2=y^2+w^t xx^t w-2yx^t w. \tag{3}$$

Taking the expected value of both sides:

$$E[e^2]=E[y^2]-w^t E[xx^t]w-2E[yx^t]w. \tag{4}$$

This expression can be simplified by defining the input correlation matrix, $R=E[xx^t]$, and the cross correlation matrix $P=E[yx]$. Utilizing these definitions in Eq. 4 results in an expression for the Mean Square Error (MSE)

$$MSE=E[e^2]=E[y^2]+w^t Rw-2P^t w, \tag{5}$$

which shows that the error squared is a quadratic function of the tap weight vector w. A plot of a MSE function, known as an error performance surface, is shown in Fig. 2 using a tap weight vector length of two. The MSE is plotted on the vertical axis while the horizontal axes represent possible values of the first and second elements of the two element tap weight vector. When the tap weight vector contains more than two elements the performance surface becomes a hyperparaboloid. The point at the minimum value of the parabolic performance surface corresponds to the optimal tap weight vector values. In this application this point is the best estimate of the actual impulse response of the physical system being investigated.

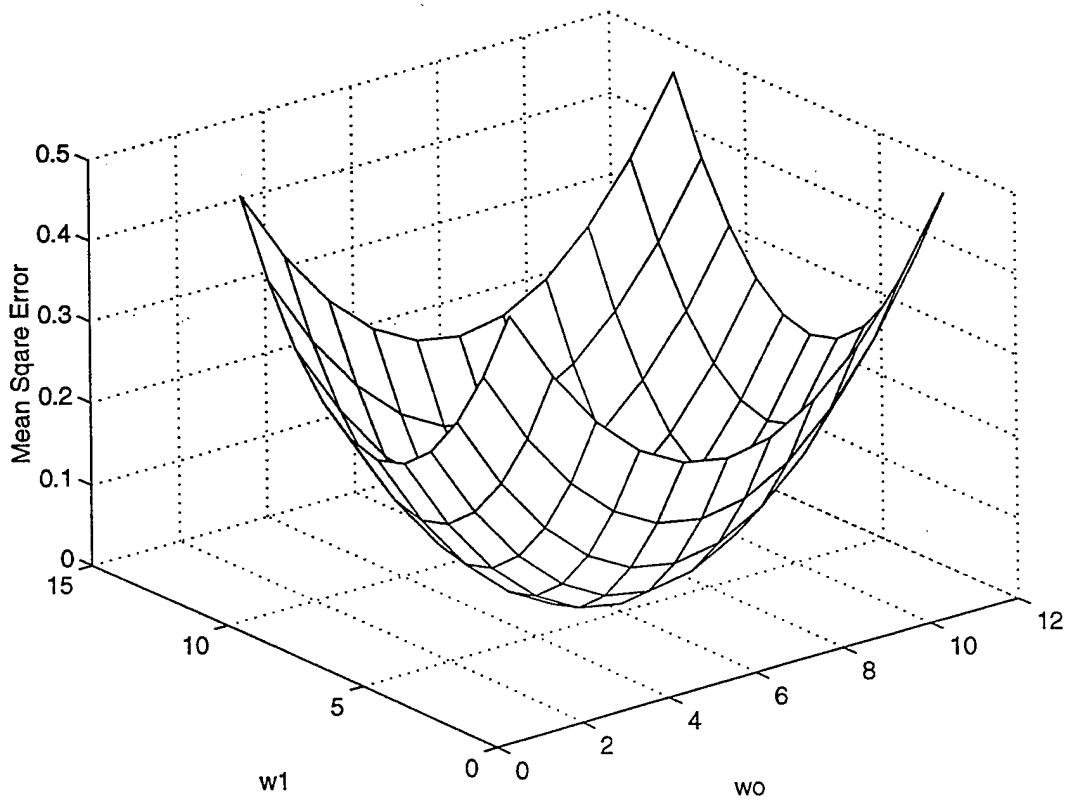

Figure 2 Error Performance Surface for Tap Weight Length = 2

In order to find this minimum value of the performance surface where error is minimized, the least mean square (LMS) algorithm is used. Other methods are available but the LMS algorithm is one of the most widely used methods in adaptive filtering mainly because of its simplicity and ease of computation (the method does not require matrix inversion).

The LMS algorithm utilizes the error defined in Eq. 2. The time index, t, has been replaced with k to represent time in this digital representation of the algorithm:

$$e(k)=y(k)-w^t(k)x(k).$$

By using $e(k)^2$ from Eq. 3 as an estimate of the mean square error in Eq. 5 the gradient can be estimated by:

$$\nabla e^2=[\partial e/\partial w]^2 =2e[\partial e/\partial w]=-2e^tx, \tag{6}$$

where $\partial e/\partial w=-x^t$ from Eq. 2.

This equation is then used in a steepest descent type of algorithm for determining the adaptive filter coefficients:

$$w(k+1)=w(k)+u(-\nabla e^2)x(k), \tag{7}$$

where u is a positive step size parameter that controls the rate of convergence to the optimal filter tap weights. Combining Eq. 6 and Eq. 7 results in

$$w(k+1)=w(k)+2ue(k)x(k). \tag{8}$$

This equation is the basis of the LMS algorithm. It does not require inversion, multiplication or squaring of a matrix.

B. INFINITE IMPULSE RESPONSE AND FINITE IMPULSE RESPONSE FILTERS

Finite Impulse Response (FIR) filters utilize current and past values of the system input to predict system output. In a FIR implementation of an adaptive filter, system output values are utilized only as the desired output signal. In Infinite Impulse Response (IIR) filters, the tap weight vector operates on current and past values of both input and output values of the system in addition to using the system output as the desired signal. This means that in an IIR filter in this application, both x(k) and y(k) are multiplied by the tap weight vectors to produce ye(k) where k is the discrete time index. For example in an FIR filter:

$$ye(k) = [x_1 \ x_2 \ x_3 \ \ldots \ x_L] \ [w_1 \ w_2 \ w_3 \ \ldots \ w_L]^t,$$

whereas in an IIR filter the estimated output is determined from x(k) and y(k):

$$ye(k)=x^t(k)\, w(k) + y^t(k)\, w'(kt),$$

where w'(k) is an additional weighting vector for the system output values. In a discrete time system this would be represented by:

$$ye(k) = [x_1 \ x_2 \ x_3 \ldots x_L \ y_1 \ y_2 \ y_3 \ \ldots \ y_L]^t \ [w_1 \ w_2 \ w_3 \ldots w_L \ w'_1 \ w'_2 \ w'_3 \ \ldots w'_L].$$

Stability is an important consideration in IIR filters because they may become unstable due to the presence of a denominator term in their transfer function [Ref. 8]. They may also have nonquadratic error surfaces or error surfaces containing local minimums. It is for these reasons that IIR filters are seldom utilized in conjunction with the LMS algorithm. However, as will be discussed in the results section, IIR filters offer a performance improvement without stability problems for system identification of the nondispersive mechanical systems investigated in this project.

C. MISADJUSTMENT

Misadjustment is the ratio of actual mean square error to the mean square error that would be present if the filter coefficients were optimal (at the bottom of the parabolic error performance surface). Because the LMS algorithm is continually refining the adaptive filter tap weight vector, the MSE fluctuates about the minimum point on the error performance surface after the filter has converged (convergence meaning that the tap weight vector has adjusted itself to values corresponding to the minimum of the error surface). As shown in reference 4, misadjustment is linearly proportional to both the convergence parameter u and the tap weight vector length L.

As u gets bigger, the LMS algorithm tends to converge faster due to the larger step size. Once the algorithm converges on a minimum error, further iterations cause the solution to move erratically about the minimum point. A small u will minimize the magnitude of these fluctuations about the minimum MSE but will slow the initial convergence to this minimum.

As L increases, the effect of a given size step down the performance surface also increases. When L is increased (more terms added to the estimated impulse response) the fluctuations around the minimum MSE have a larger effect on the filter coefficients and thus increase the misadjustment error.

D. WAVES IN BARS AND PLATES

This project used adaptive filters to identify the impulse response of vibrating bars, plates and rings. Both dispersive and nondispersive vibrations were studied.

In the first part of the experiment, torsion, flexural and longitudinal waves were selectively excited electromagnetically in plastic and aluminum rods [Ref. 5]. The rods were in a free-free condition (both ends free to move). Torsional or longitudinal excitation results in harmonic modes of vibration described by:

$$f_n = nc/2l \tag{9}$$

n=mode number=1, 2, 3...

$c=c_T$ (torsional wave speed) or c_l (longitudinal wave speed)

l=length of bar

Flexural waves are dispersive, which means that their wave speed is a function of frequency. Free-free boundary conditions were again used which resulted in nonharmonic modes of vibration given by: [Ref. 5]

$$f_n=\pi n^2 c_l k/8l^2 \tag{10}$$

n=(3.0112, 4.9994, 7.0000, 9.0000...)

k=radius of gyration = radius/2 for a round bar

l=bar length

Wave propagation speed is frequency dependent for dispersive waves with wave speed given by:

$$c=(2\pi f c_l k)^{1/2} \tag{11}$$

E. THEORETICAL OPTIMUM IMPULSE RESPONSE

The optimal frequency response (which is the Fourier transform of the impulse response) for single input, single output systems is conventionally computed from [Ref. 7] :

$$H(f) = G_{xy}(f) / G_{xx}(f) \tag{12}$$

$G_{xy}(f)$ = one sided cross spectral density

$G_{xx}(f)$ = one sided auto spectral density

As will be discussed in the results section, adaptive filters produced a better estimate of the impulse response of the simple systems investigated here than an impulse response determined by taking the inverse FFT of the result of Eq. 12.

III. EXPERIMENT

A. ELECTRODYNAMIC TRANSDUCTION

Electrodynamic transduction was utilized to generate longitudinal, torsional and flexural waves in circular bars. [Ref. 6]

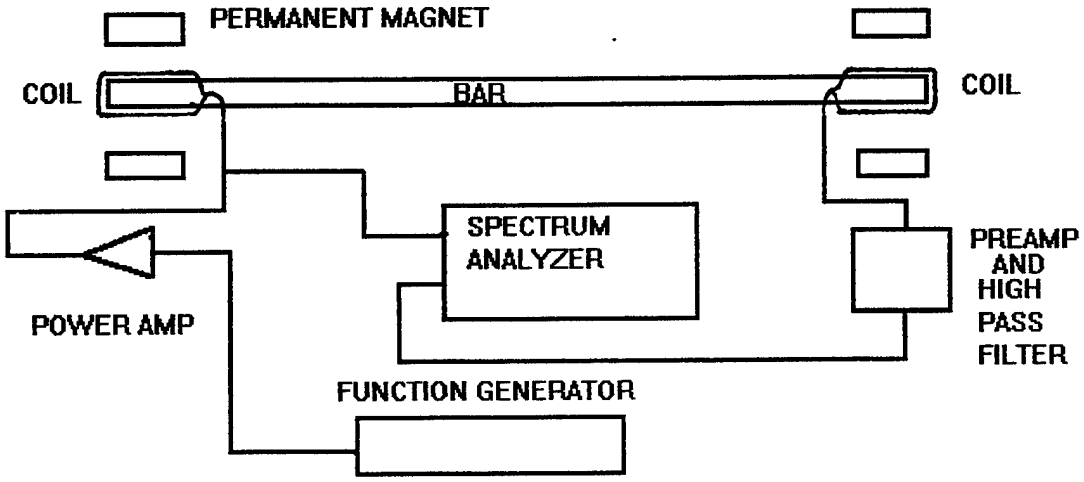

Figure 3a Electrodynamic Transduction

A coil of about 20 turns of thin wire was wrapped around each end of the bar. Each end of the bar was then placed in a magnetic field created by the two permanent magnets on each end. As shown in Fig. 3b and 3c, by changing the relative orientation between the permanent magnets and the coil, different types of waves can be induced in the bar. For example, to induce torsional waves in the bar the rod is arranged such that the coil is lying flat in the horizontal plane perpendicular to the magnetic field between the two magnets on either end. Using the right hand rule this will cause the long sides of the coils (which are rigidly attached to the bar with epoxy) to oscillate up and down when an AC current is passed through the coils. [Ref. 6]

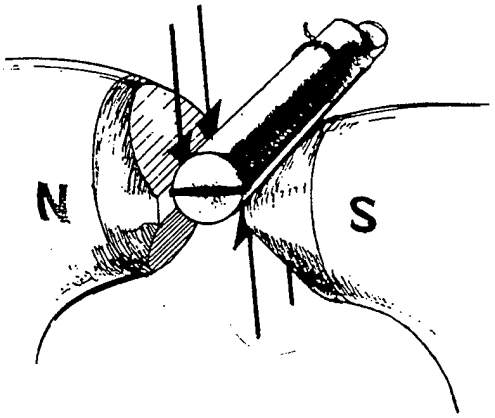

Orientation of the coil and magnet pole pieces for the transduction of the torsional mode. The arrows indicate the magnitude and direction of the electromagnetic forces on the two dominant sections of the coil for a given phase of driver current. The forces produce the moment that excites the torsional oscillations.

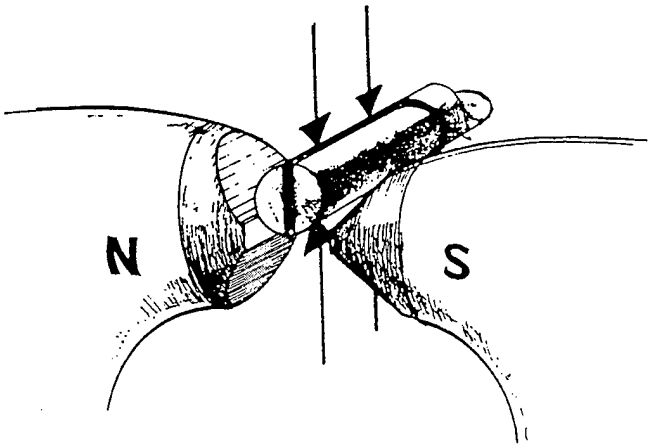

Orientation of the coil and magnet pole pieces for the transduction of the flexural mode. The arrows indicate the magnitude and direction of the electromagnetic forces on the two dominant sections of the coil for a given phase of driver current. The lower section of the coil is in the stronger region of the magnetic field and hence exerts a greater force on the bar than the upper section of the coil, as indicated by the shorter arrows above the bar. This leads to a net force that excites the flexural mode.

Figure 3b Magnet-Coil Orientation for Torsion and Flexural Waves (From Ref. 6)

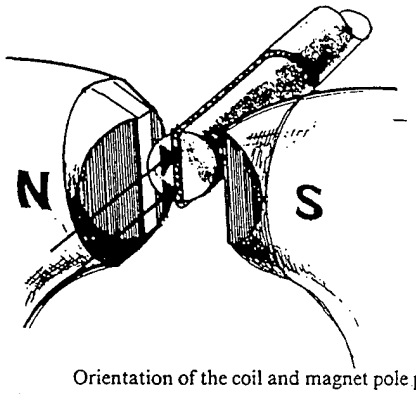

Orientation of the coil and magnet pole pieces for the transduction of the longitudinal (extensional) mode. Note that the pole pieces have been rotated by 90° to concentrate the magnetic field just beyond the end of the bar. The arrows indicate the magnitude and direction of the electromagnetic forces on the dominant section of the coil for a given phase of driver current. Since this section of the coil at the end is shorter than the other sections used to drive the torsional and flexural modes, it is useful to reduce the amount of stray magnetic field that links the other portions of the coil if the longitudinal mode spectrum is not to be "polluted" by the presence of the torsional modes.

Figure 3c Magnet-Coil Orientation for Longitudinal Waves (From Ref. 6)

The input signal into the input coil and the amplified output signal were recorded using LabVIEW [Ref. 11] on a Macintosh Quadra 800 computer with the input and output sampled at 48 kHz. The input signal into the bar was provided by the HP 3562A spectrum analyzer or a function generator.

Plastic bars (Nylon) provided the best results for the purposes of this project because of its low Young's and Shear moduli. This results in a lower sound speed in the material which makes analysis easier on the short pieces of material (less than a meter long) that were used in this investigation. Copper and aluminum bars were tried but analysis was difficult because the waves traveled down the bars too fast.

Torsion waves were found to be useful for investigating nondispersive waves because they have a lower sound speed than longitudinal waves. This is due to the fact that a material's shear modulus is in general smaller than its Young's modulus.

B. SHAKER TABLE

In a second experiment, flexural waves were generated in a horizontal 2.54 X 2.54 X 68 cm plastic bar by displacing one end of the bar vertically with a shaker table. The input signal was taken from an accelerometer bolted directly on the shaker table. The output was measured with an accelerometer bolted vertically on the free end of the bar. The small difference in motion between the input accelerometer mounted on the shaker table and the end of the bar which was attached to the shaker table was considered to be part of the impulse response to be modeled by the adaptive filter.

C. PIEZOELECTRIC TRANSDUCER

In the final experiment, two small, home made piezoelectric transducers were superglued to the sides of a 62.4 X 15.2 X 1.5 cm aluminum plate. It was necessary to use both a low noise preamplifier and a power amplifier for the output because of the low sensitivity of these PZT transducers. As before, the input and output signals were recorded using LabVIEW. One of the disadvantages of using the PZT

transducers is that they tend to attenuate low frequency signals. This is because the transducers have little of the mass loading which would be required for them to operate at low frequencies. [Ref. 13]

The accelerometers were also used to excite waves in an aluminum ring. The PZT input and output transducers were attached about 90° apart on a 2 cm thick, 10 cm wide aluminum ring with a 17 cm mean diameter. The ring was made out of two half cylinders which were bolted together. This boundary between the half cylinders had the effect of adding more propagation paths to the system (the reflected and transmitted paths at the boundary). The ring was suspended from ring stands with flexible cord to eliminate boundary effects that would be present with the ring laying on a table.

As will be discussed in the results section, it was often necessary to damp the mechanical systems to lower their Q factor. This was accomplished by wrapping the material with vinyl electrical tape and then with damping tape (a heavy metal tape). The electrical tape provided a compliance while the damping tape provided both compliance (the sticky part of the tape) and mass (the metal part of the tape).

The adaptive filters used to estimate the impulse responses of the mechanical systems were implemented in Matlab [Ref. 12] using the system input and output data imported from LabVIEW.

IV. RESULTS

A. ADAPTIVE FILTER PERFORMANCE FOR SYSTEMS EXCITED WITH PERIODIC SIGNALS

The input signal used in most of the experiments was white noise. Whenever any type of periodic signal was used for input (sine wave, square wave or sawtooth wave) the adaptive filter predicted the system output nearly perfectly for both dispersive and nondispersive systems. Figure 4a demonstrates this for the case of a damped (Q=8) plastic bar being driven with torsion waves at its resonant frequency of 1.5 kHz. Figure 4b demonstrates excellent performance for the same plastic bar being driven with flexural square waves at a flexural resonant frequency of 580 Hz.

It is interesting to note the response of the plastic bar to the square wave input. A square wave can be thought of as a summation of sine waves. Because the bar acts as a low pass filter only the lowest frequency component of the square wave (a 580 Hz sine wave) is present at the output. Higher components are not likely to land on other flexural resonances because of the nonharmonic nature of dispersive flexural waves as shown by Eq.10. Also note that in this example an adaptive filter tap weight vector only 24 samples long is adequate to produce an estimated output with low error even though the output is a sine wave that has a period equivalent to about 82 samples.

The adaptive filters converged (convergence meaning that the tap weight vector has adjusted itself to a steady value near the bottom of the performance surface) in less than 16000 iterations for all of the experiments, which corresponds to 0.33 seconds at a 48 kHz sampling rate.

Convergence times were determined by observing the adaptive filter behavior for steady sinusoidal inputs. This ensured that the impulse response of the physical system remained the same during the experiment. Using a random noise input may have excited different types of waves in the bar such as torsion waves and flexural waves. Figure 5a shows the fractional error for sine wave induced flexural waves in a plastic bar converging in about 3500 iterations (equivalent to 73 ms at a 48 kHz sampling rate)

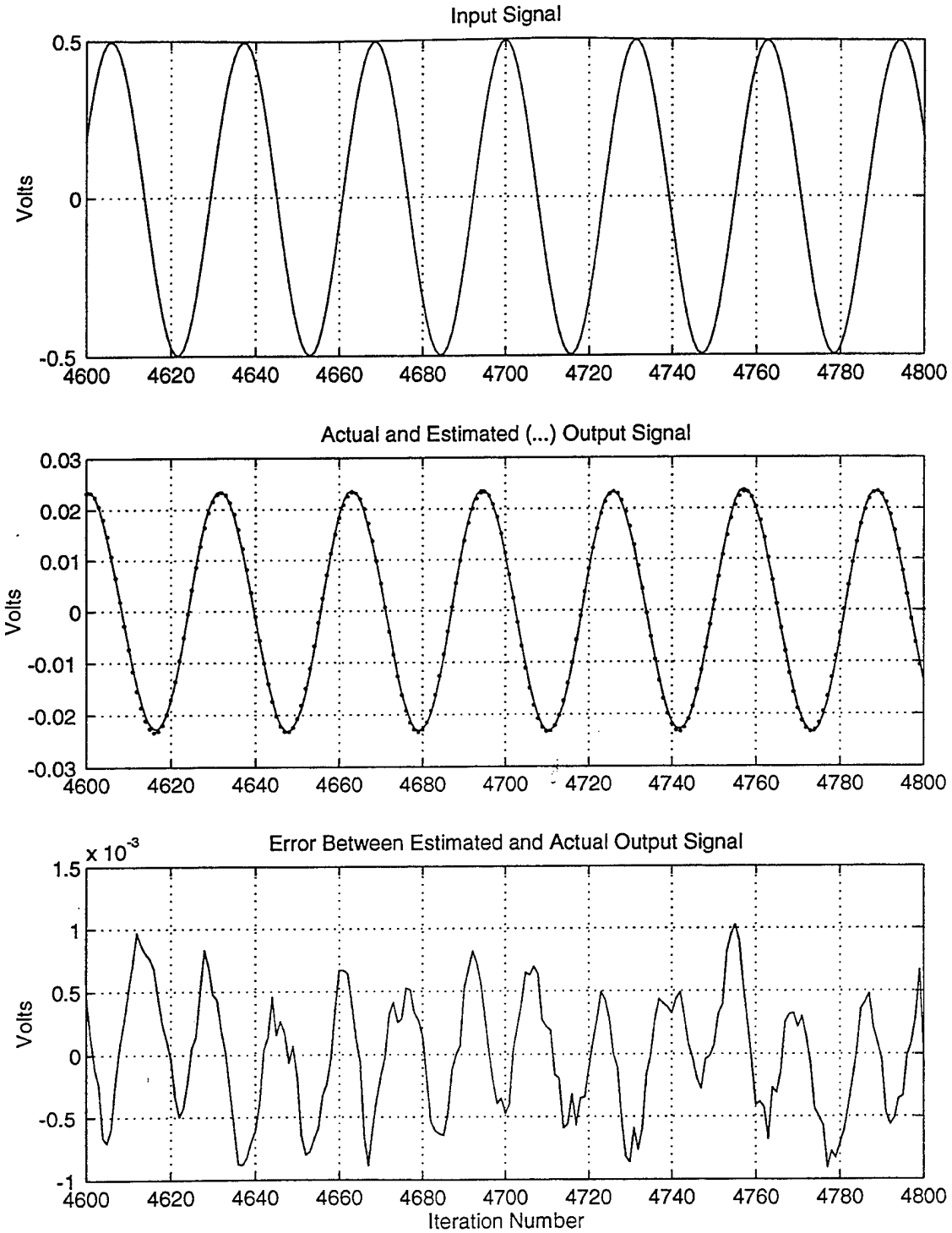

Figure 4a 1.5 kHz Torsion Wave in a Plastic Bar

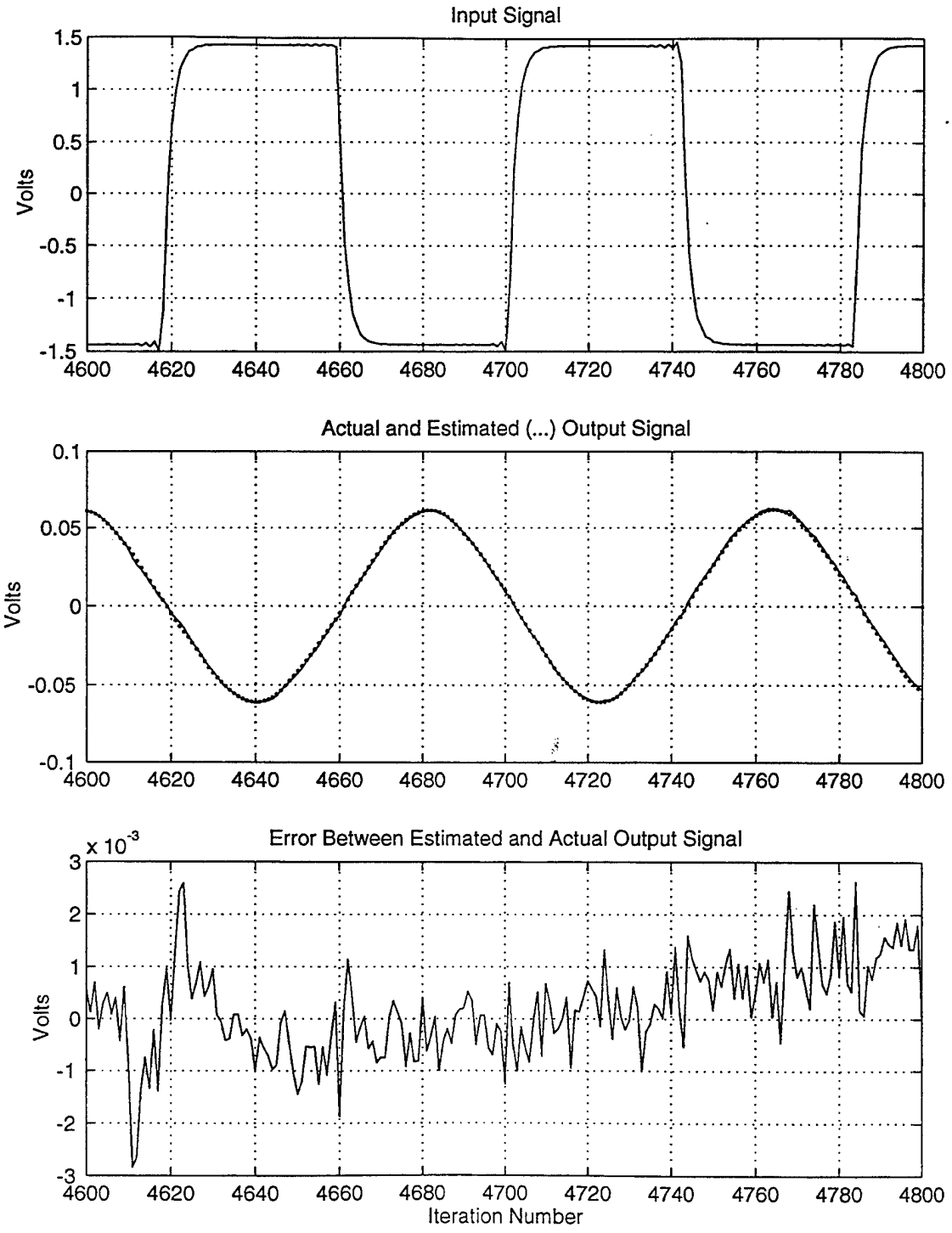

Figure 4b 580 Hz Flexural Wave in a Plastic Bar

to a steady error that is due primarily to misadjustment. The fractional error is the difference between the estimated and actual outputs divided by the average rms value of the actual output. The convergence can also be seen by plotting the log of the fractional error to see where the error settles on a steady value as in Fig. 5b.

Figure 5c shows the convergence of a 580 Hz torsional square wave in the same plastic bar which is below resonance for a torsion wave. Convergence occurs in about 8000 iterations (167 ms at a 48 kHz sampling rate). Figure 5e shows the convergence using the damped aluminum ring being excited at 8.08 kHz which is its first resonant frequency. Convergence takes much longer, at least 250 ms, apparently because of the multiple propagation paths present in the ring, all of which must be modeled by the tap weight vector. The high Q of the ring (about 1000 even after damping) also slows convergence because vibrations in high Q systems decay slowly resulting in many passes of the signal being present at the output transducer. These two factors also account for the poor performance of the algorithm in finding an impulse response that accurately predicts system output.

The convergence times for waves in the plastic bar can be compared to several characteristic times associated with the bar. The one way propagation time for both torsional and flexural waves from the input coil to the output coil is one of these characteristic times. Another is the relaxation time of the oscillating bar which is the time necessary for the motion of the freely oscillating bar to decay to 1/e of its initial amplitude. Relaxation time is computed from [Ref. 14]

$$\tau = 2Q/\omega_o \tag{13}$$

where ω_o is the natural frequency in radians. A third characteristic time is the "characteristic dispersion time" which is derived in the appendix. This is the time required for the second mode to dephase by $\pi/2$ with respect to double the frequency of the fundamental mode as a result of the dispersion. These characteristic times are shown below for the 0.444 m long plastic bar using measured values for torsional and longitudinal wave speeds of 1047 m/s and 1425 m/s respectively (longitudinal wave speed is used in Eq.10 in the calculation of flexural wave speed).

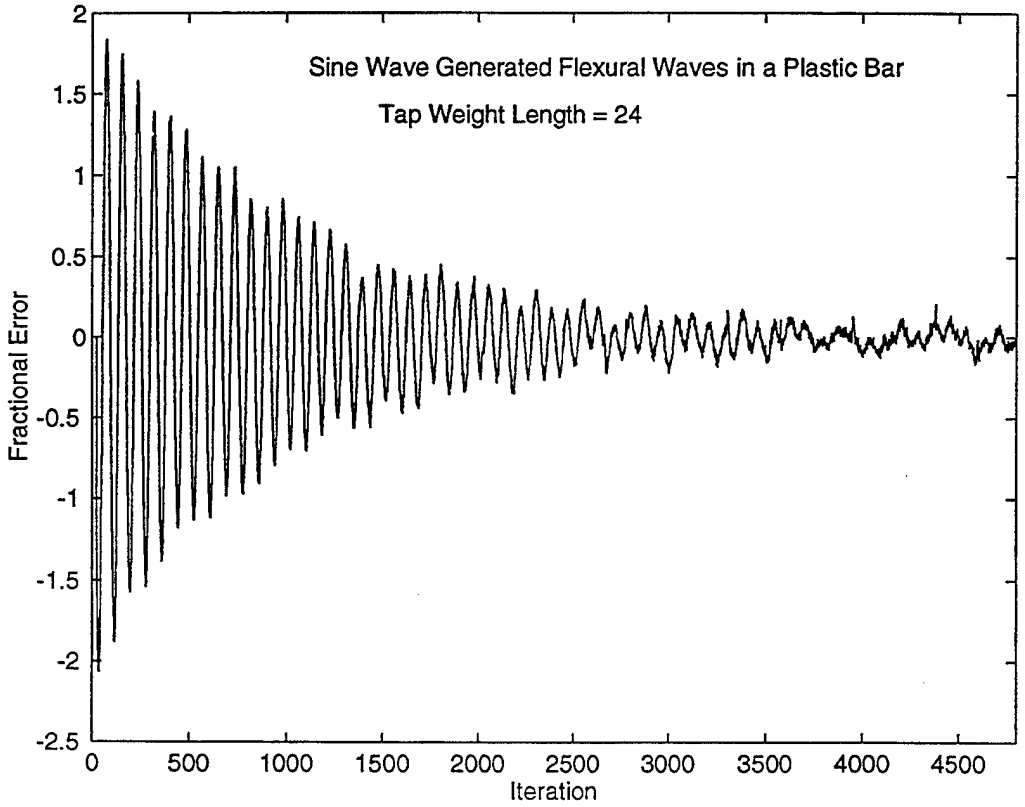

Figure 5a Adaptive Filter Convergence for Flexural Waves in a Plastic Bar

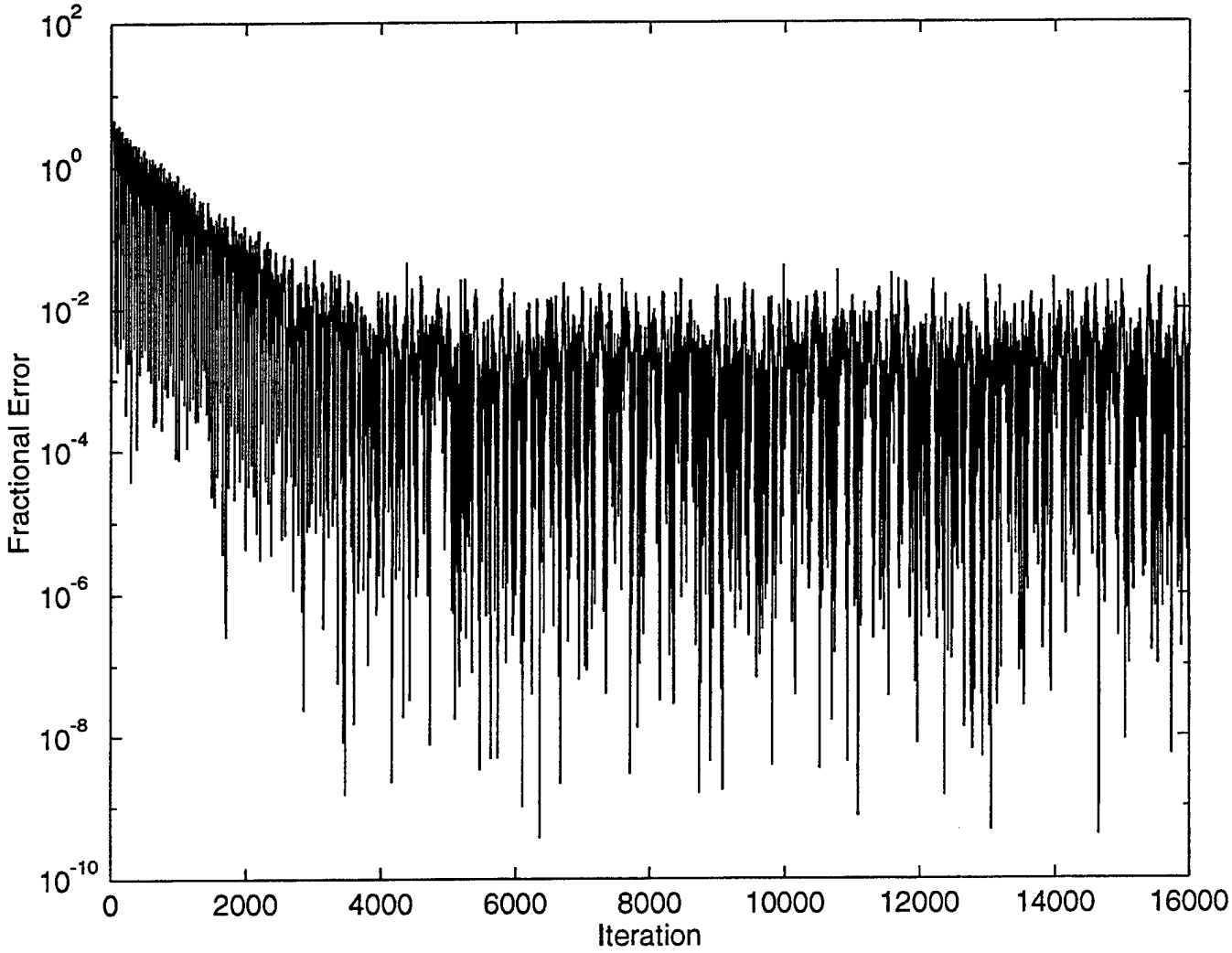

Figure 5b Adaptive Filter Convergence for Flexural Waves in a Plastic Bar (Log Plot)

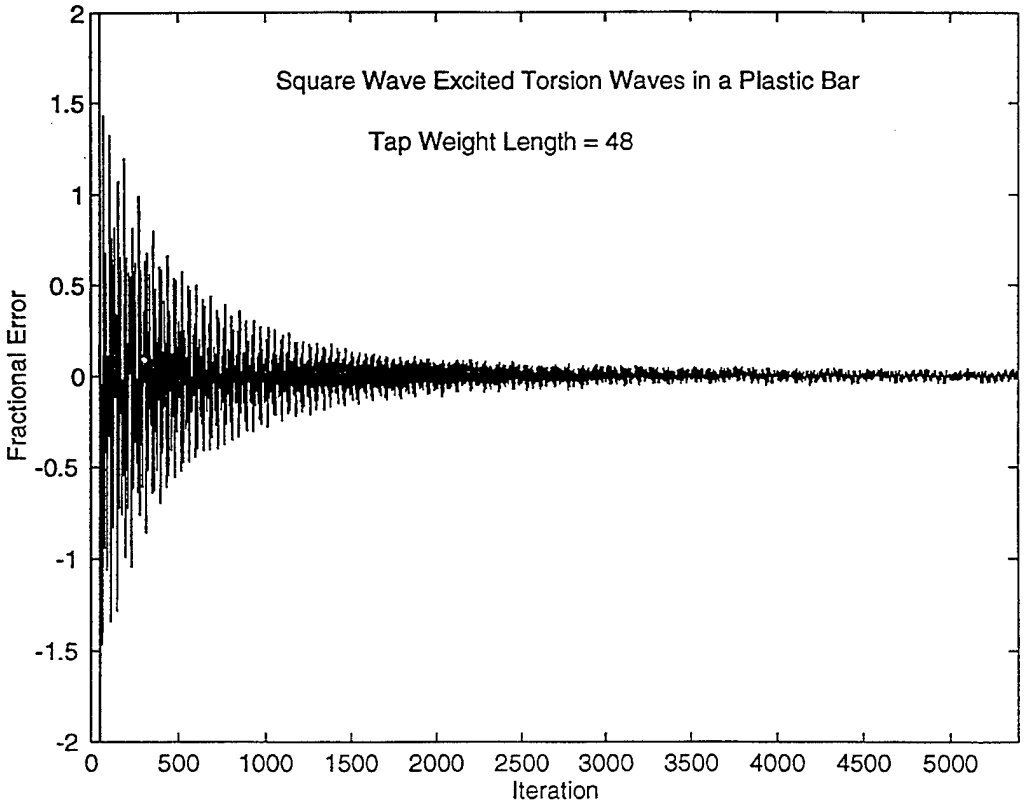

Figure 5c Adaptive Filter Convergence for Torsion Waves in a Plastic Bar

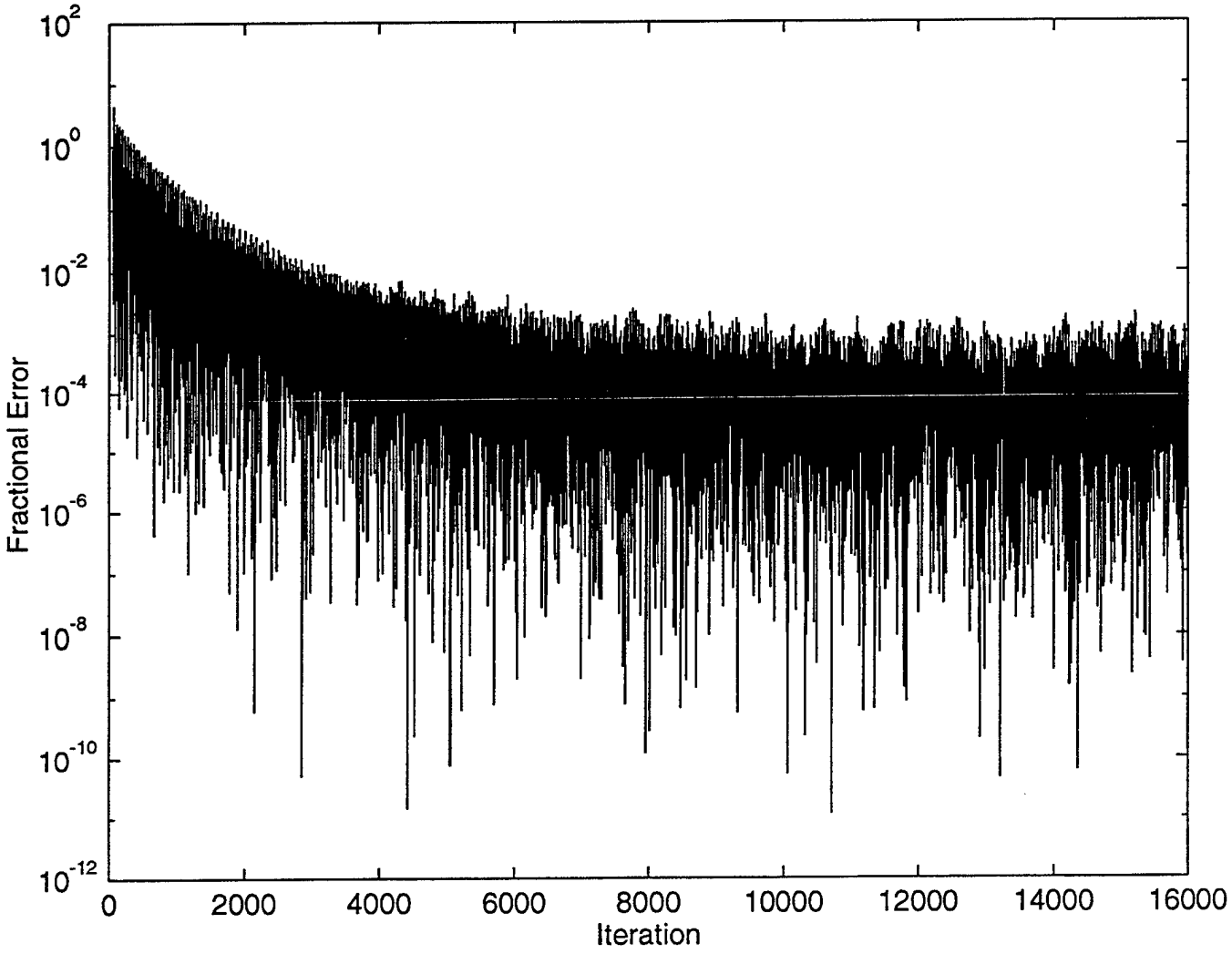

Figure 5d Adaptive Filter Convergence for Torsion Waves in a Plastic Bar (Log Plot)

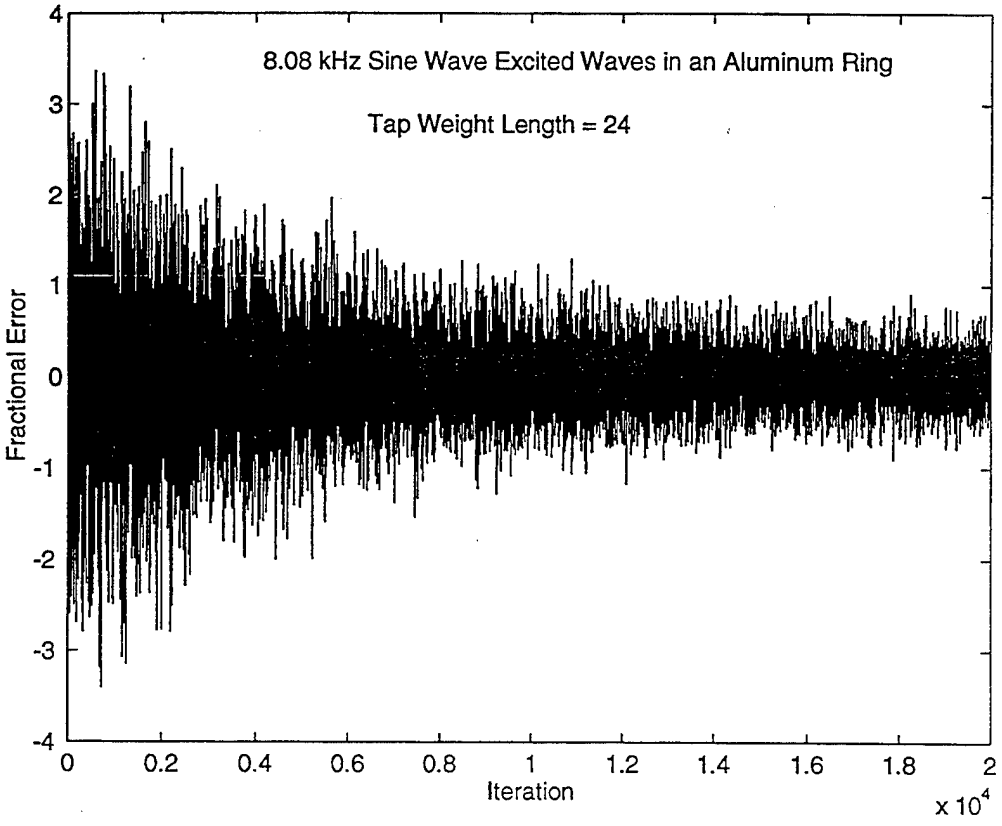

Figure 5e Adaptive Filter Convergence for Waves in an Aluminum Ring

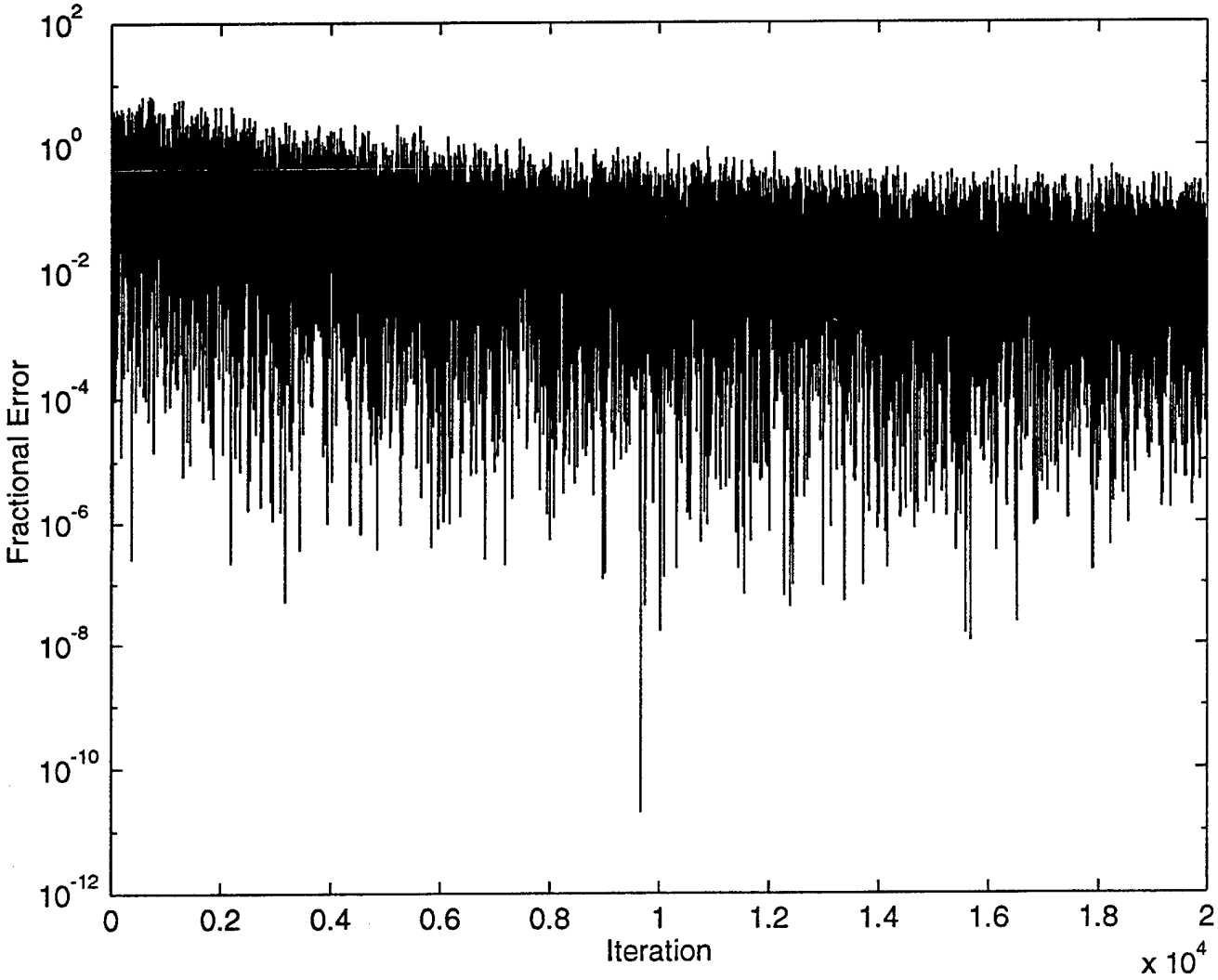

Figure 5f Adaptive Filter Convergence for Waves in an Aluminum Ring (Log Plot)

Wave Type	Time to Converge to Steady State	Propagation Time	$\tau_{decay}=2Q/\omega_o$	Characteristic Dispersion Time
Torsional	42 msec	0.416 msec	2.3 msec	3.4 sec
Flexural	73 msec	10.8 msec	27.3 msec	4.0 msec

Table 1 Characteristic Times of the Plastic Bar

It is difficult to come up with a meaningful propagation time for the aluminum ring because of the multiple propagation paths present in the ring. However, the input and output transducers were 0.07 m apart which resulted in a 0.013 ms propagation time for longitudinal waves traveling in a direct path between the two transducers.

B. TAP WEIGHT VECTOR CONVERGENCE

The value of the step size parameter u is important in ensuring that the adaptive filter will converge to a steady tap weight vector solution for systems with time varying impulse responses. The basis of the LMS algorithm is Eq. 8:

$$w(k+1)=w(k)+2ue(k)x(k).$$

The step size u determines how big a jump down the error performance surface is taken during each iteration. The jump must be small enough to ensure that the solution (the tap weight vector w) can reach the bottom of the parabolic performance surface. (As the parabolic error performance surface flattens near its minimum, big jumps on the surface during each iteration are likely to miss the optimal solution) On the other hand, u must be large enough to allow the filter to converge on a good tap weight vector solution as quickly as possible.

Since u must not be too small nor too large, it is convenient to have some way of adjusting u to a value that will ensure convergence in a reasonable amount of time even if the impulse response changes. This was accomplished by using a u of variable size. The size was adjusted as a function of the error between predicted and actual output with each iteration [Ref. 10]:

$$u(t) = u_o(1-\beta\gamma e^{-(1/2)\gamma error^2}), \quad (14)$$

where β and γ are constants that control the rate of convergence. Note that u has units of inverse power. This function is plotted in Fig. 6a using a variety of values for β and γ. A value of u_o of 0.05 was found to work well for the simple mechanical systems investigated here. Reducing u prevents the solution (the tap weight vector values) from moving too far around the performance surface minimum after convergence and producing erroneous results. Since this choice of u is a function of error squared, the step size will increase when the error is large, such as when the physical system changes, which is desirable to aid in quick adaptation to a new optimum tap weight vector solution.

Figure 6b demonstrates the ability of the u to change when the impulse response changes. In this case the transfer function was altered at sample 2400. At this point the output data record was multiplied by a factor of 20 leaving the phase unchanged (the actual physical system was not altered). Eq. 14 was utilized to adjust u to quickly find a new impulse response to reduce the squared error. Fig. 6c demonstrates what happened when a constant u was used and the impulse response changed at the 2400th sample. The error squared grew very quickly because the tap weight vector of the adaptive filter was not able to converge onto the bottom of the error performance surface.

C. TAP WEIGHT VECTOR LENGTH AND INPUT LAG TIME

The adaptive filter algorithm used in this application uses the system input x(t) and the error signal between the desired signal y(t) and the adaptive filter output ye(t) to determine w(t), the estimated impulse response of the mechanical system. Because propagation of the vibration wave from the input of the mechanical system to the output takes a certain amount of time, the algorithm is using information from mismatched times. From Eq. 8 the changes in w(t) are proportional to the product of the output error, derived from outputs due to an input signal at a previous time, and the system input from the present time. Thus it should be possible to delay the input signal x(t) by:

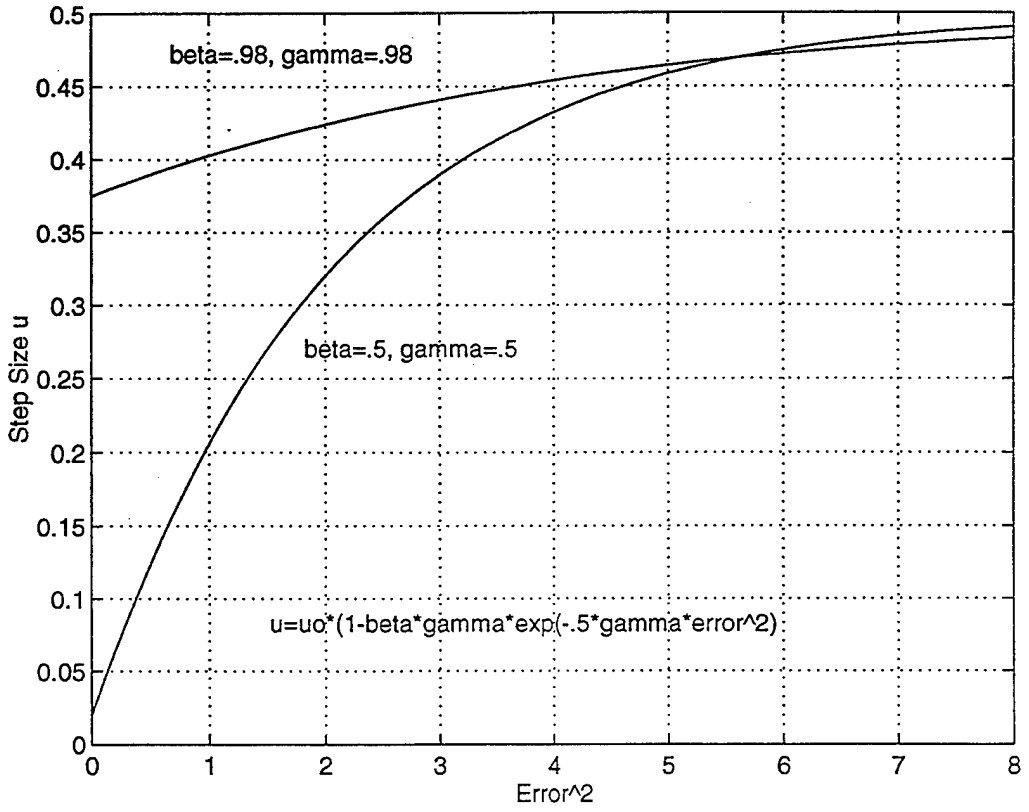

Figure 6a Variation of u with Error^2 for u_0=.05

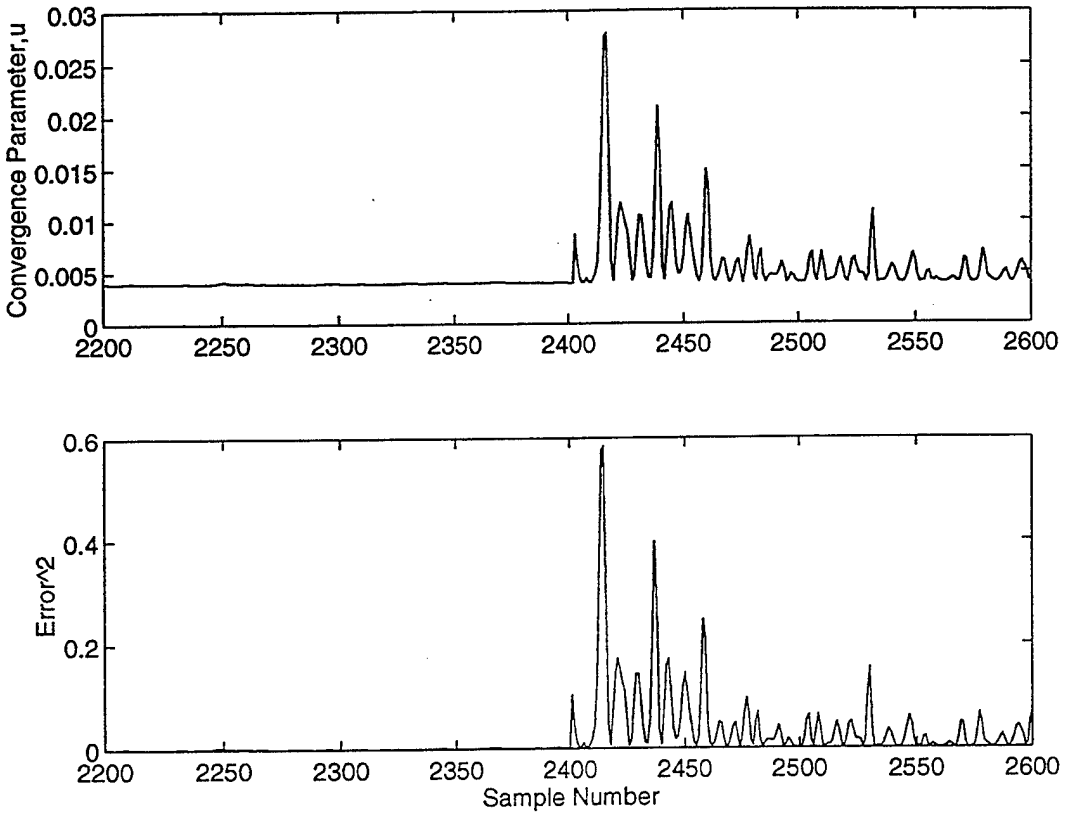

Figure 6b Response to a Changing Impulse Response for a Variable u

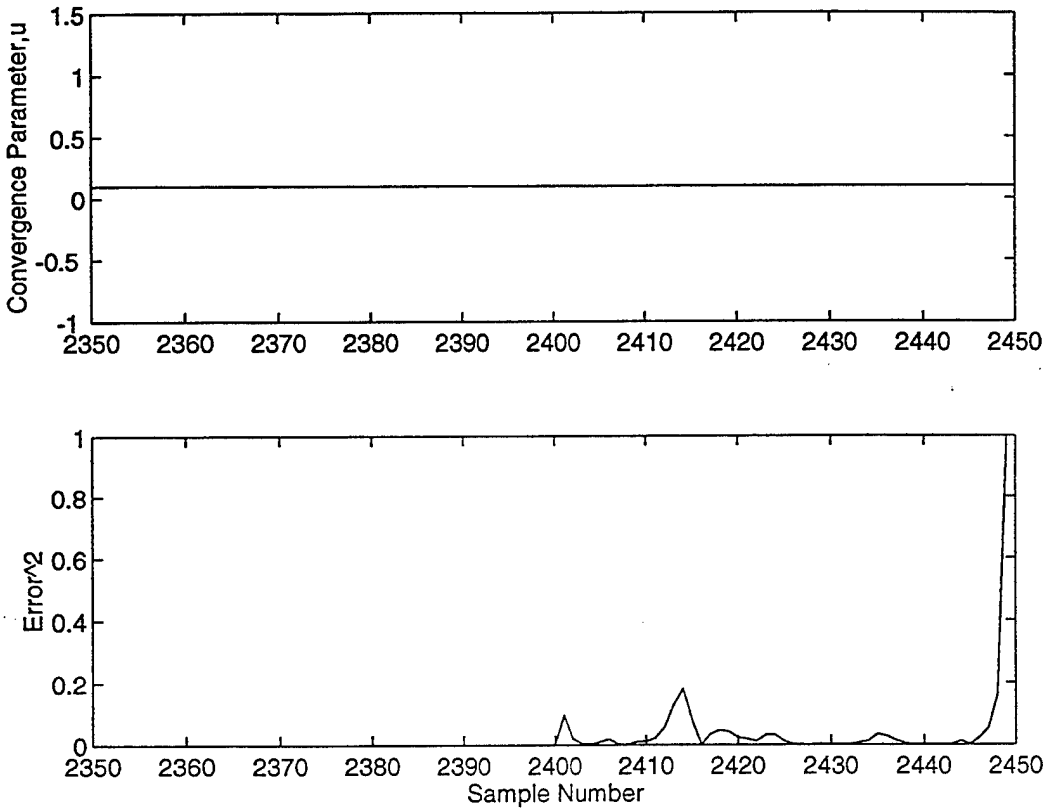

Figure 6c Response to a Changing Impulse Response for a Fixed u

delay = Propagation Distance / Wave Speed in Medium (15)

before it is used in Eq. 8 to improve performance.

The propagation time in each of the different systems was measured using the HP 3562A Spectrum Analyzer. In the following example torsion waves were electromagnetically induced in a damped plastic bar with a broadband noise input. The analyzer first determined the complex frequency response of the system and then took the inverse FFT of it to determine the impulse response. The different torsional modes of the system can be seen in the frequency response on the far left of the plot on the bottom of Fig. 7. The upper part of Fig. 7 shows the impulse response. Because the impulse response is proportional to the cross correlation between the input and output, peaks in the impulse response correspond to the arrival time of a wave at the output. [Ref. 7] The first pulse represents the propagation time of the initial torsion wave traveling down the bar and gives the propagation time for a wave traveling once down the length of the bar. The second peak represents a wave traveling down the bar, reflecting off the output end, traveling back towards the input end of the bar and then back to the output end of the bar. The rest of the peaks represent further reflections from the ends of the bar, their magnitudes progressively decreasing as the wave attenuates and spreads out in time due to dispersion (Even though the waves were generated as nominally nondispersive torsion waves, some dispersion occurs because of the non ideal end conditions on the bar due to the imperfect electromagnetic coil transducers.)

The first peak begins at 424 μsec which means that the torsion waves travel down the bar in this amount of time. Since the bar is 0.444 m long this results in a torsional wave speed of:

$$0.444 \text{ m} / 424 \text{ μsec} = 1047 \text{ m/sec}$$

This corresponds to a theoretical value for torsional wave speed determined from:

$$c = (G/\rho)^{1/2}$$

$$c = (0.4 \text{ X } 10^{10} / 1200)^{1/2} = 1080 \text{ m/sec}$$

Where G is the shear modulus of the bar.

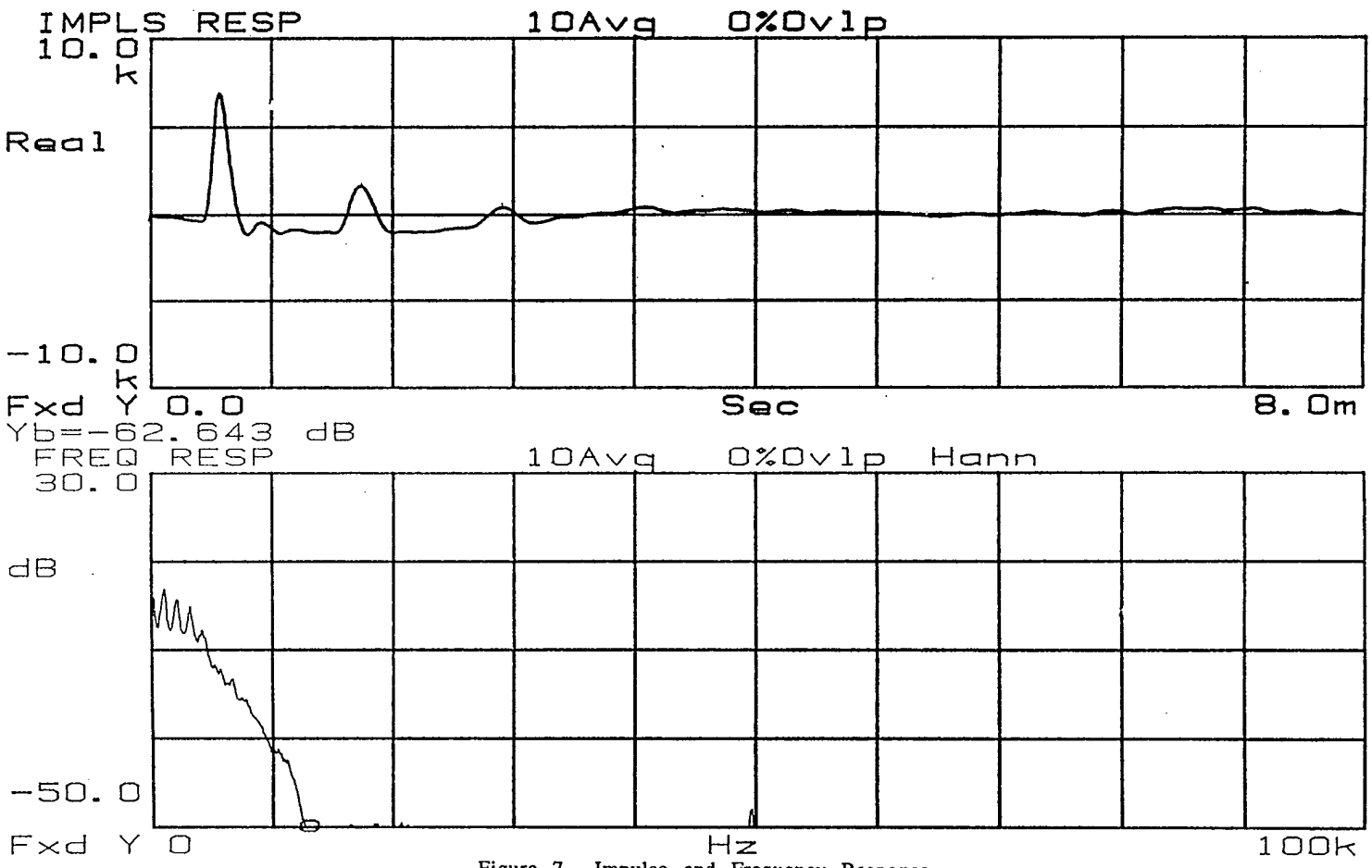

Figure 7 Impulse and Frequency Response

Figure 8a shows that delaying the x(t) input to the adaptive filter as suggested by Eq. 16 can improve the performance of the adaptive filter when modeling torsional wave propagation in the damped plastic bar. This plot shows that when x(t) is delayed by about 20 samples the adaptive filter performance improves for four different tap weight vector lengths. The average error shown is for the last 200 iterations of a 4800 iteration experiment since this represents filter performance after it has converged on a solution. At the 48 kHz sampling rate used in data collection, 20 samples corresponds to 411 microseconds, which is close to the propagation time measured using the impulse response.

Figure 8b shows a similar result for a 0.92 meter long undamped aluminum rod through which torsion waves are propagating. The aluminum has a much higher Q than the damped plastic bar (600 for aluminum and 8 for the plastic) which could be why the plots are not as smooth as the one for plastic. Torsional wave speed in the bar is 2980 m/s which results in an optimal delay of 0.92m / 2980m/s = 0.31 milliseconds. This corresponds to an expected minimum error at a lag of about 15 samples at a 48 kHz sampling rate which is close to the results seen in Fig. 8b.

As the tap weight vector length L is increased, the minimum error decreases as does the amount of lag necessary to achieve the best filter performance. This is because as the tap weight length increases the input does not have to be delayed as much for the tap weight vector to account for the propagation time of vibrations through the system. This is demonstrated by the "minimums" in the error squared stretching out towards zero lag time as the tap weight vector length is increased. Each element of the tap weight vector represents 1/fs (fs=sampling rate) seconds of time.

Figures 9a and 9b show results for dispersive flexural waves generated in a plastic bar for L=128 and L=228 respectively. The minimums occur after a longer lag because the wave speed for flexural waves is slower than for torsional waves in this material. The minimum at a lag of about 300 samples corresponds to the travel time of the first flexural mode of the bar (the slowest of the flexural modes). This lag time can be predicted by computing the first resonant frequency from Eq. 10:

$$f_1 = \pi\,(2187)\,(0.00318)\,(3.0112)^2 /\ 8\,(0.444)^2 = 126 \text{ Hz},$$

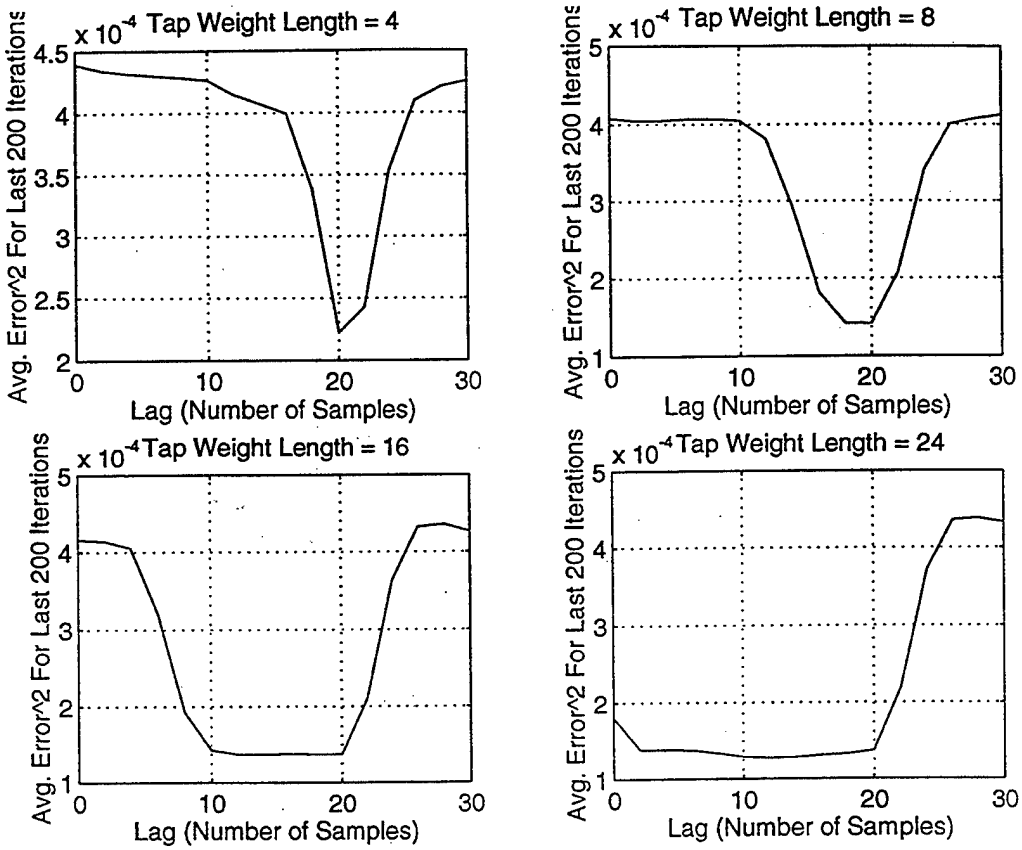

Figure 8a Error vs. Input Lag in a Plastic Bar in Torsion

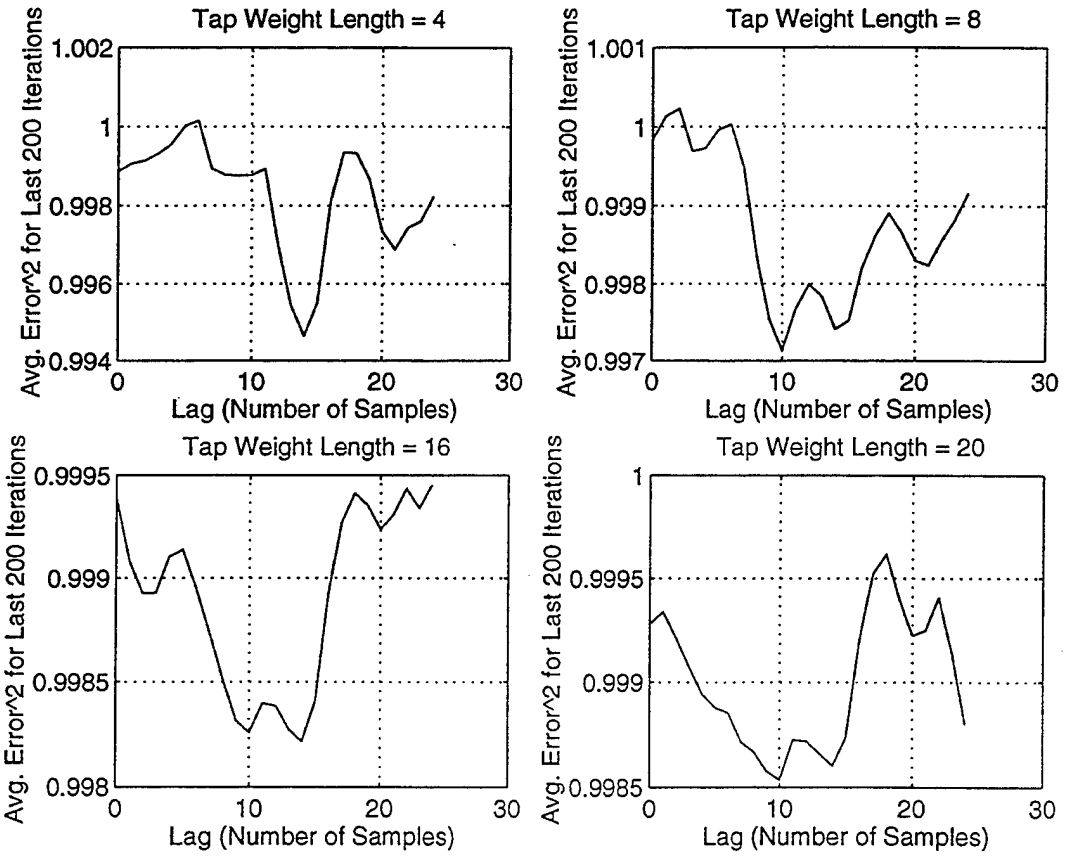

Figure 8b Error vs. Input Lag for Flexural Waves in an Undamped Aluminum Bar

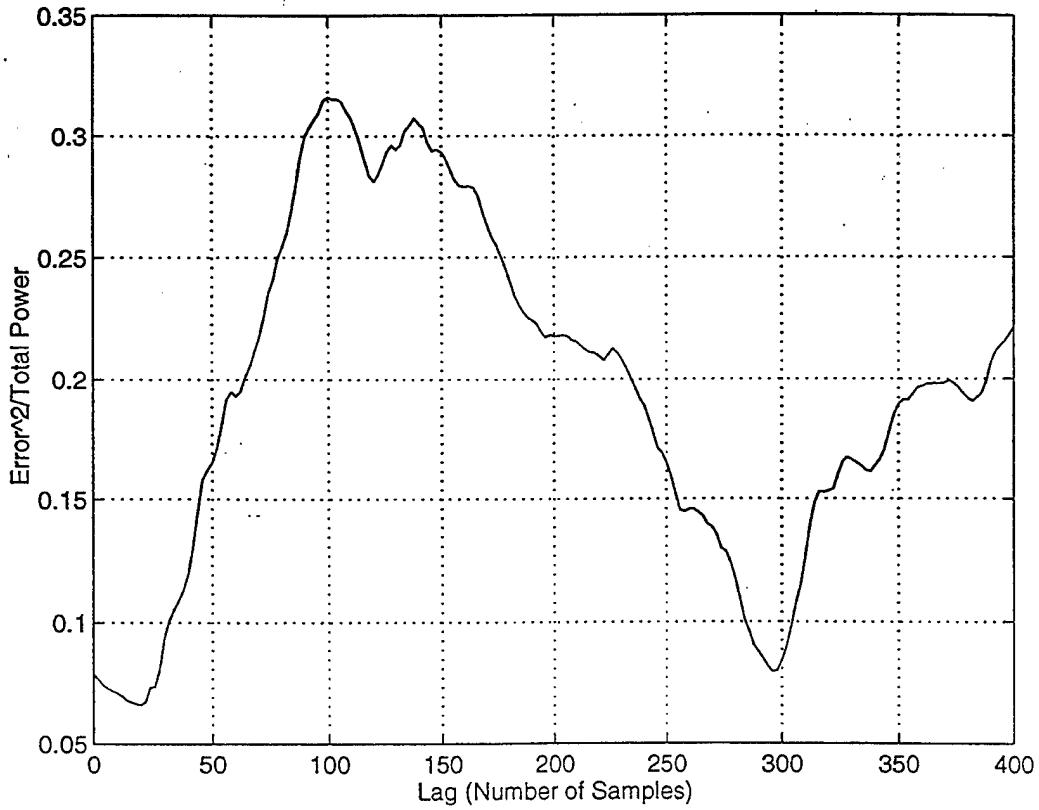

Figure 9a Flexural Wave in a Plastic Rod Showing a Minimum at Lag=300 Due to Travel Time of the Flexural Wave (L=128)

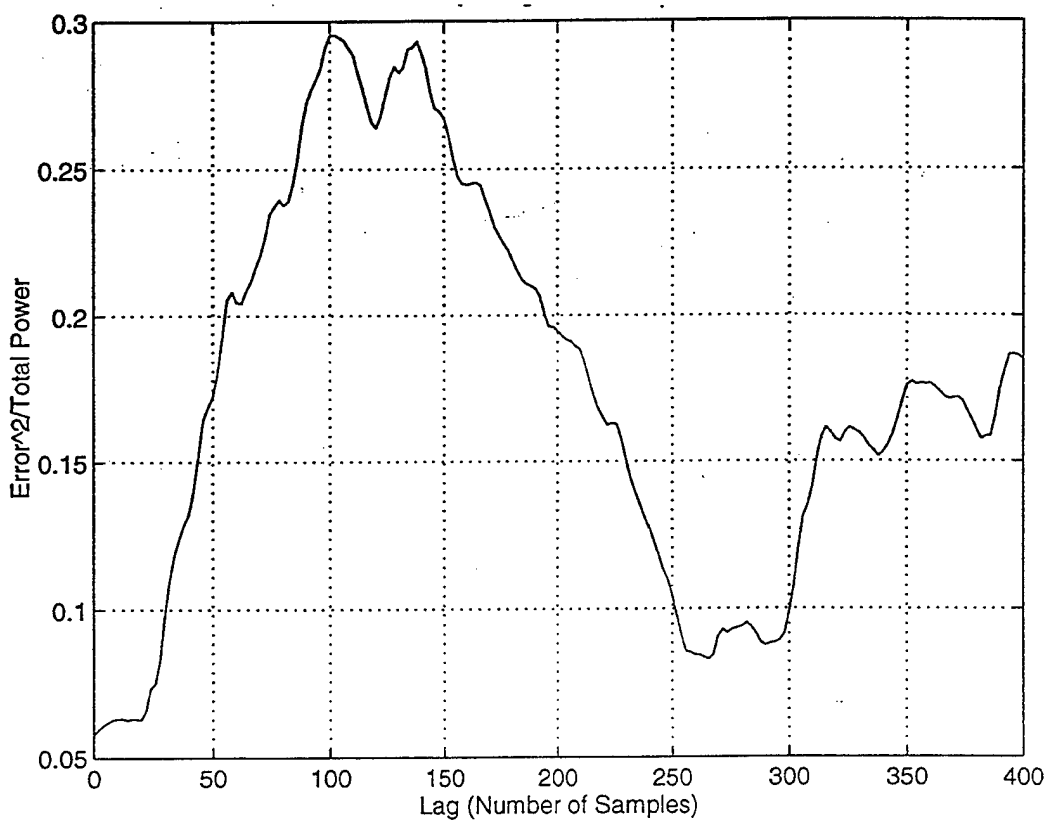

Figure 9b Flexural Wave in a Plastic Rod Showing a Minimum at Lag=300 Due to Travel Time of the Flexural Wave (L=228)

where f_1 is the frequency of the first dispersive mode using a longitudinal wave speed of 2187 m/s, a radius of gyration of 0.00318 and a length of 0.444 m. From Eq. 11 the speed of the first mode is:

$$c_1 = [2\pi\,(126)\,(0.00318)(2187)]^{1/2} = 74 \text{ m/sec.}$$

This results in a travel time that corresponds to a lag of 287 samples which is quite close to the result in Fig. 9. The error with zero lag is smaller than the value that would be expected when propagation time is taken into account because of the dispersive nature of the wave which causes it to spread out in time as it propagates. This apparently makes it difficult for the adaptive filter to model the mechanical system with a relatively short tap weight vector.

Figure 10 shows the effect of delaying the input to the adaptive filter for the case of the aluminum ring. Apparently, because of the multiple propagation paths present in the ring and its high Q (about 1100), delaying the input does not improve filter performance. The periodic nature of the result (about 3 samples between the weak minimums) does, however, correspond to the propagation time between the input and output transducers mounted on the ring. Similar results were obtained for the experiment utilizing PZT transducers mounted on an aluminum plate excited by broadband noise.

As discussed in the background theory section, tap weight length cannot continue to grow indefinitely to reduce error because of misadjustment error which is proportional to the tap weight vector length. Figure 11 demonstrates this for the case of broadband noise exciting torsional waves in the damped plastic bar. Error squared initially decreases with increasing tap weight length then increases as misadjustment error begins to dominate. The input signal x(t) was not delayed for this example. The first large drop in the error squared occurs at a tap weight length of about 20. The 20 tap weights at a 48 kHz sample rate correspond to 20 X 1/48kHz = 416 microseconds which is the propagation time for a torsional wave traveling from one end of the bar to the other. A tap weight vector more than 20 elements long is thus adequate to model the first wave reaching the end of the bar. The second large drop in the error squared occurs at a tap weight vector length of about 60 which corresponds to the wave traveling down the bar, reflecting off the end, then traveling down and back up the bar.

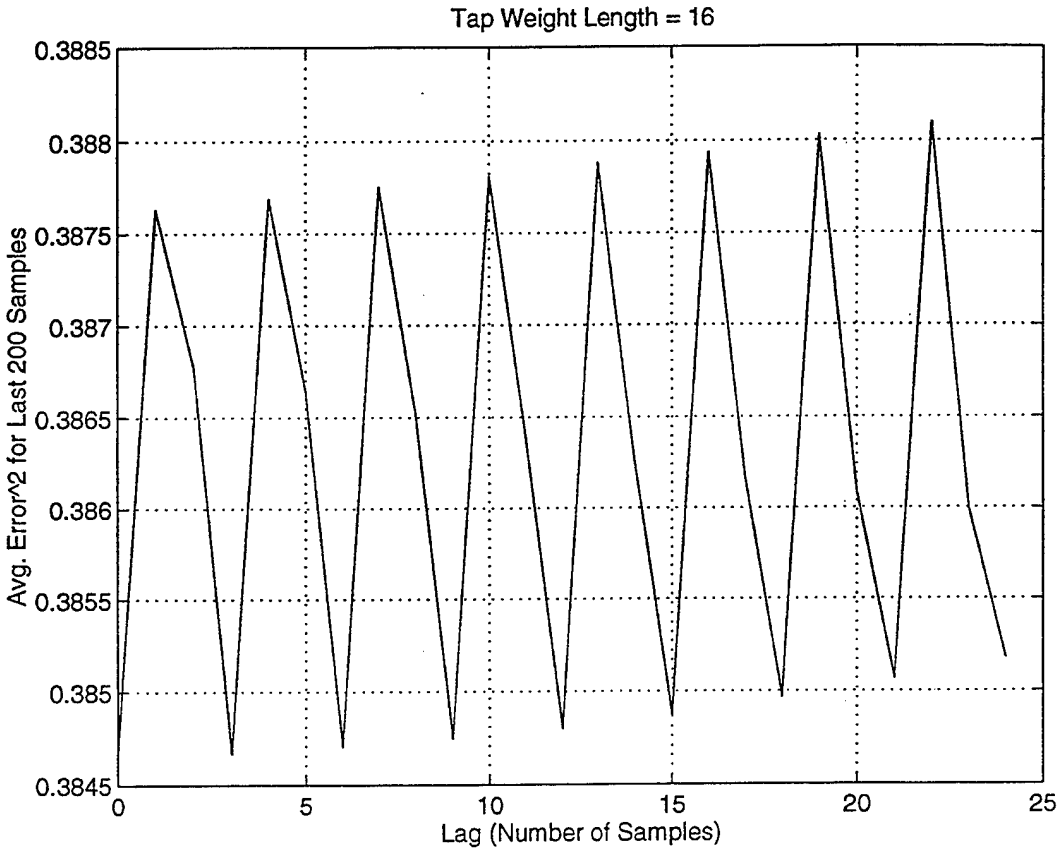

Figure 10 Error Vs. Input Lag for Waves in an Undamped Aluminum Ring (Multiple Propagation Paths)

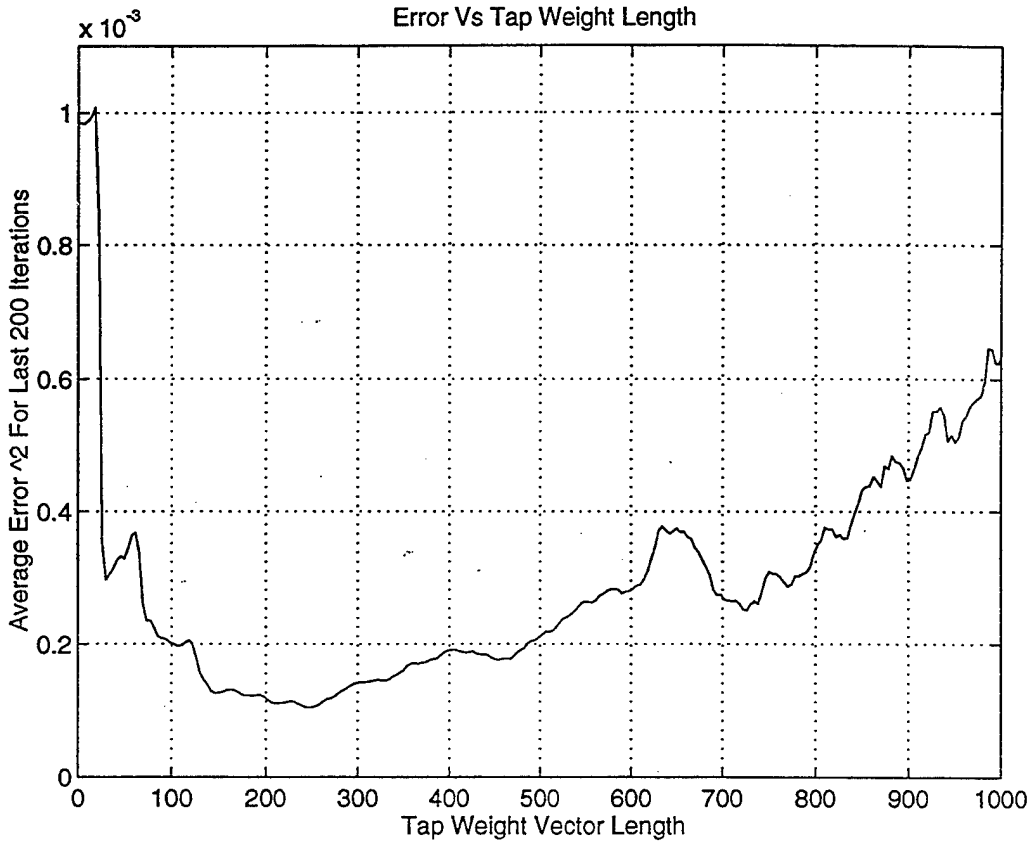

Figure 11 Error vs. Tap Weight Vector Length

When periodic inputs were used, the predicted output increased drastically as the tap weight length was increased past a certain length using both the recursive and nonrecursive filters. It was evident that this effect was due to something other than misadjustment error which causes error squared to increase about linearly with tap weight length after reaching some minimum value as shown in Fig. 11. The performance of the adaptive filter improved as the tap weight vector length L got longer until a certain value past which the filter was unable to generate a stable solution. This value of L depends on u; decreasing u increased the maximum value of L for which the adaptive filter produced a stable solution.

An example of this phenomenon is shown in Fig. 12a. A 580 Hz square wave was used to drive flexural waves in a damped plastic bar with the step size parameter u initially set to 0.05. It can be seen that increasing the tap weight vector length improved the performance of the adaptive filter until a tap weight vector length of 155, above which the adaptive filter did not produce a stable solution. When u was reduced to 0.04 in Fig. 12e-g, the filter provided a stable solution when a tap weight vector as long as 166 was used, above this value an unstable solution was again generated.

D. SYSTEM Q

Q is the quality factor or "sharpness" of a resonance. It is equal to 2π times the ratio of the energy of an oscillator at resonance to the energy dissipated per cycle. It plays an important role in the performance of the LMS algorithm because high Q systems have very sharp resonances which are described by very long impulse responses. When these impulse responses are longer than the tap weight vector, the filter is insufficient to model the physical system and large errors between predicted and actual output result.

The Q of the undamped aluminum bar was about 700 while the Q of the undamped aluminum plate was about 2800 (The Q was determined by dividing the resonant frequency by the width of the peak at its -3 dB down points). At these high Q's the filters performed quite poorly and were unable to

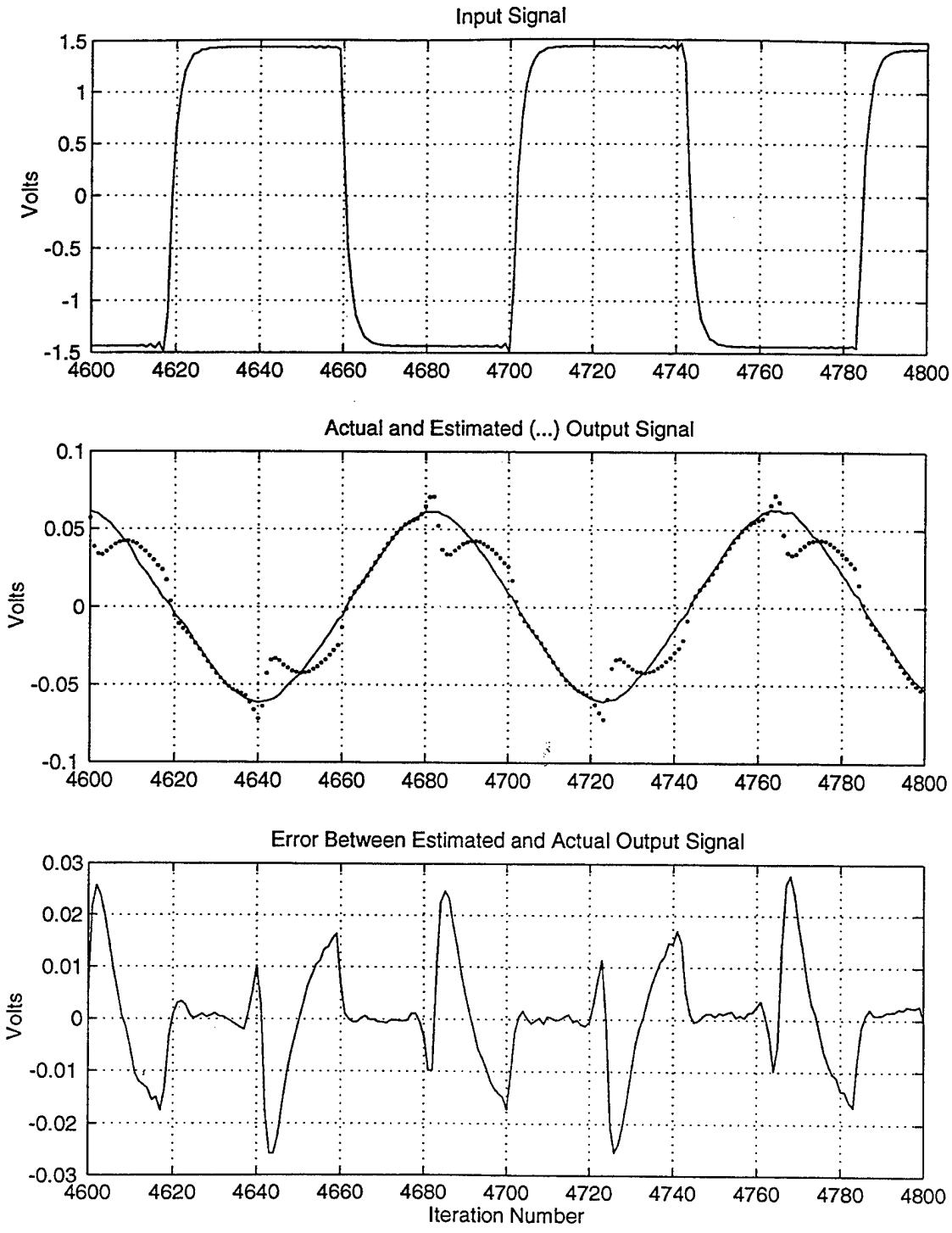

Figure 12a 580 Hz Sqare Flexural Waves in a Plastic Bar (L=24)
Initial u=0.05

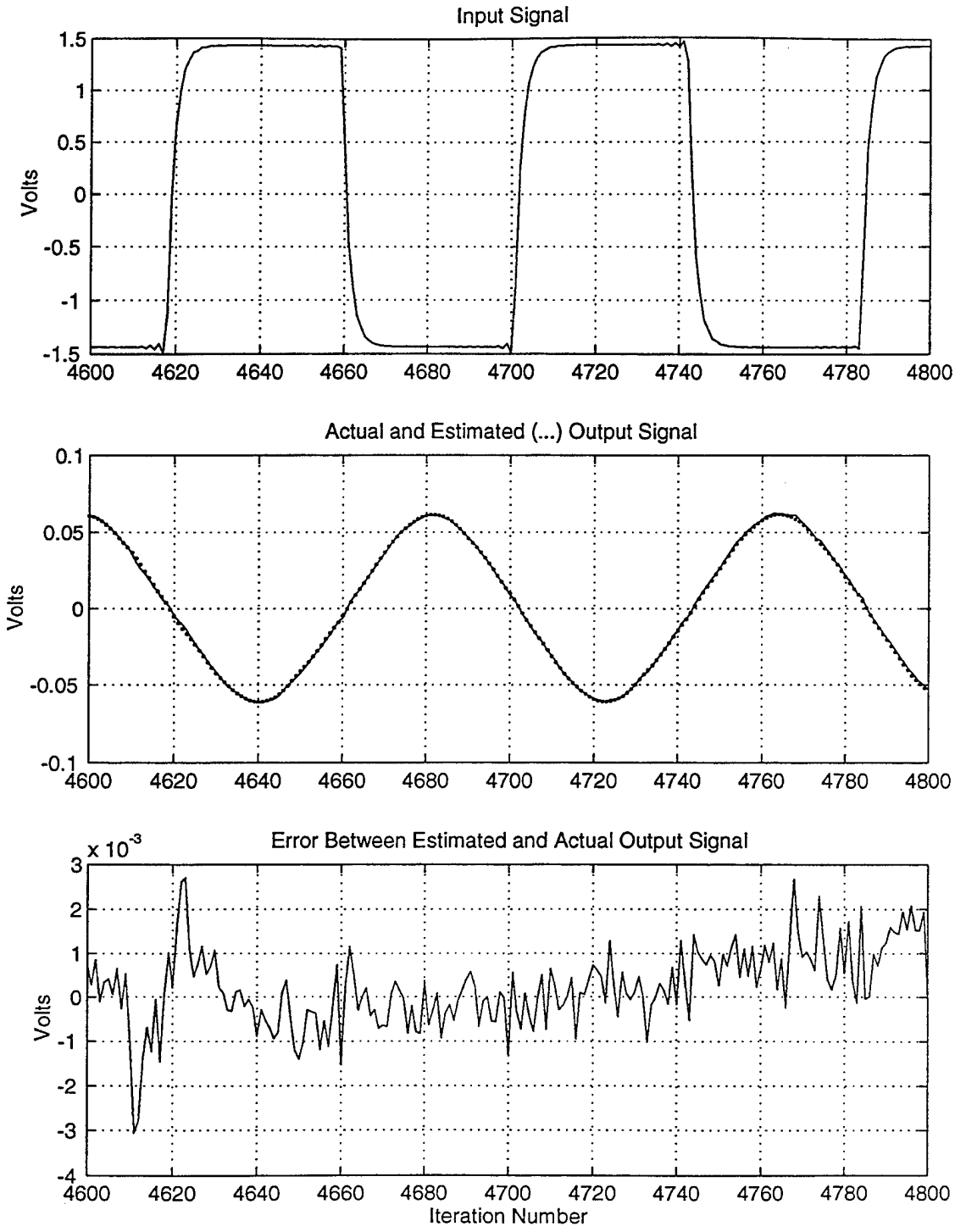

Figure 12b 580 Hz Sqare Flexural Waves in a Plastic Bar (L=72)
Initial u=0.05

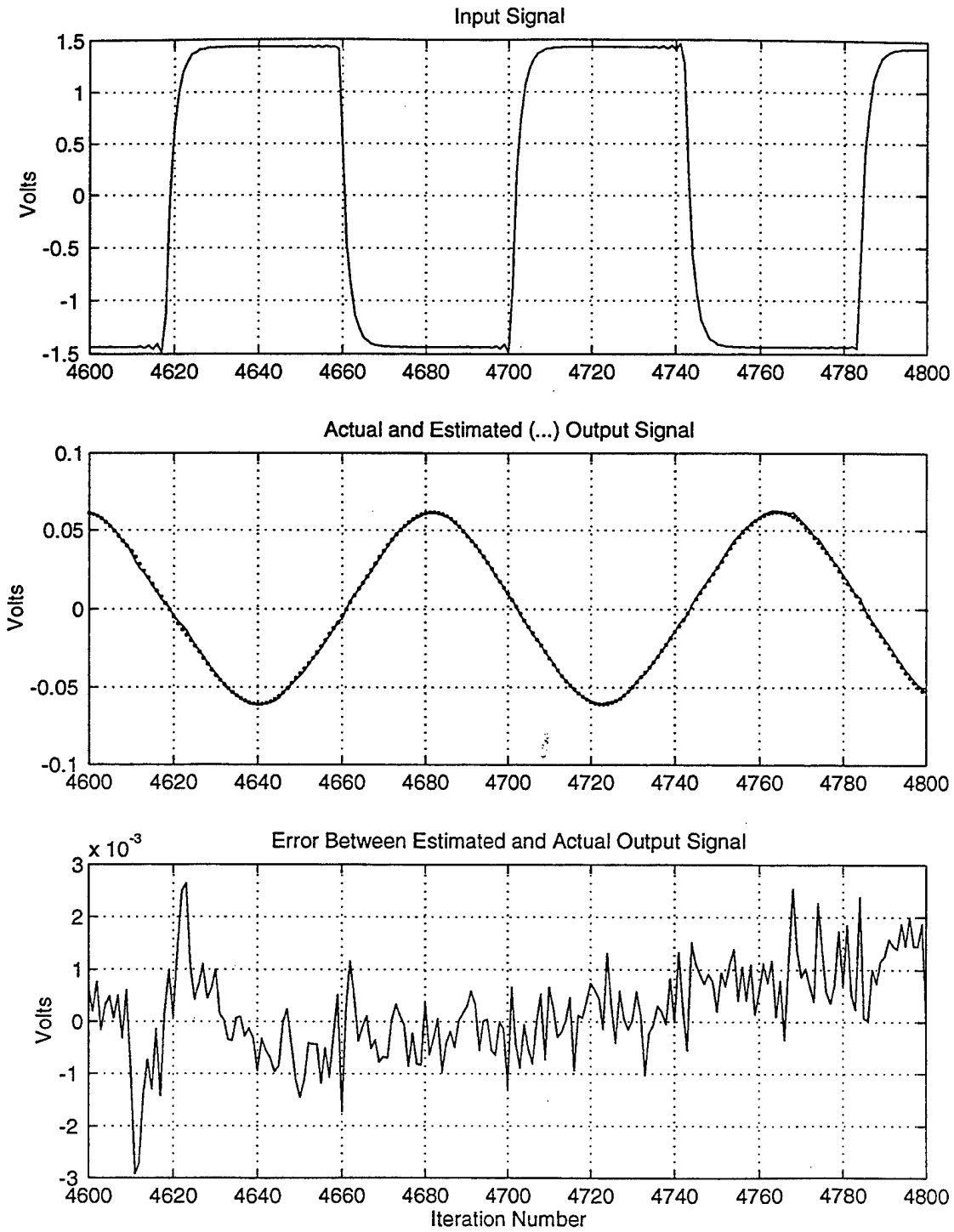

Figure 12c 580 Hz Sqare Flexural Waves in a Plastic Bar (L=155)
Initial u=0.05

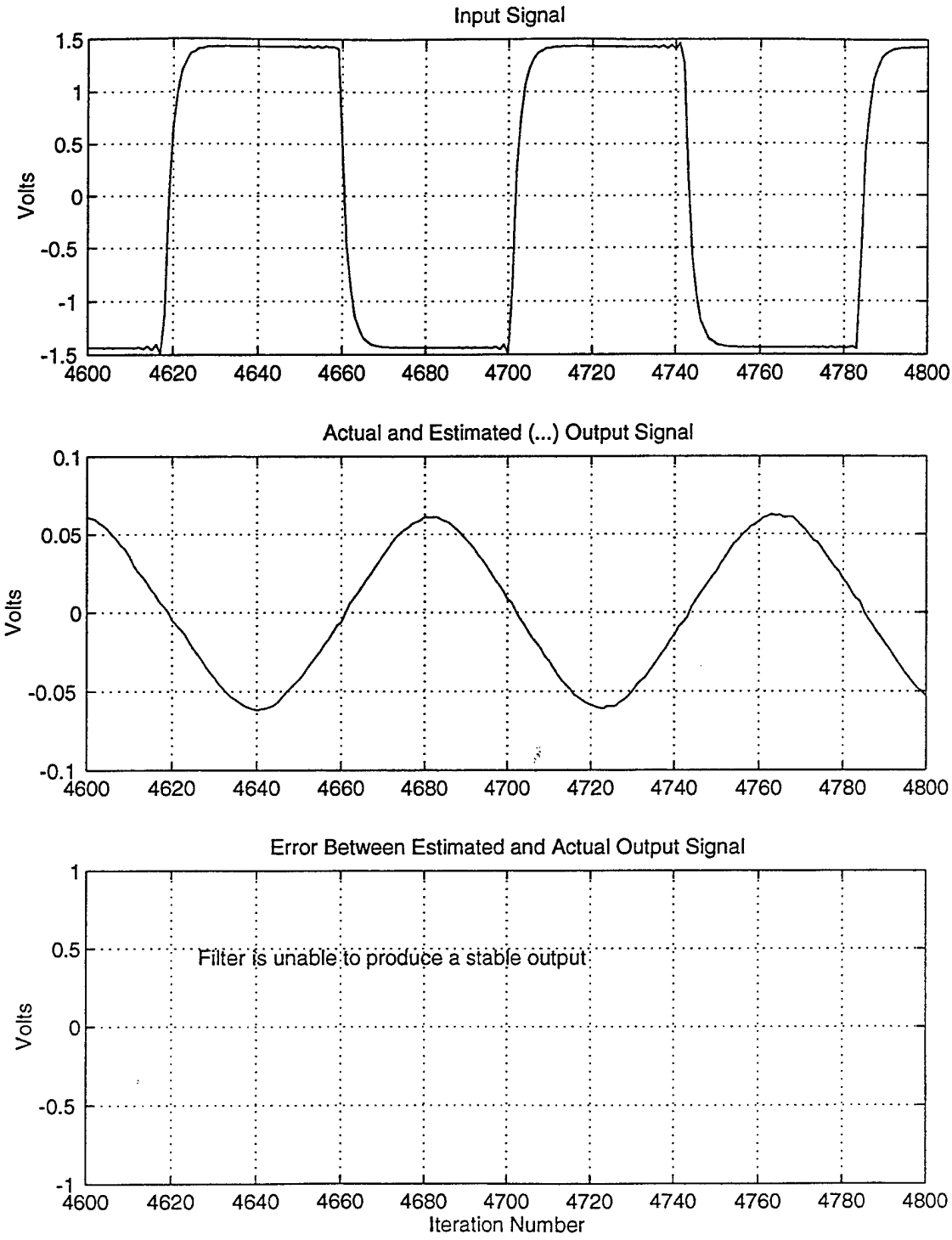

Figure 12d 580 Hz Sqare Flexural Waves in a Plastic Bar (L=156)
Initial u=0.05

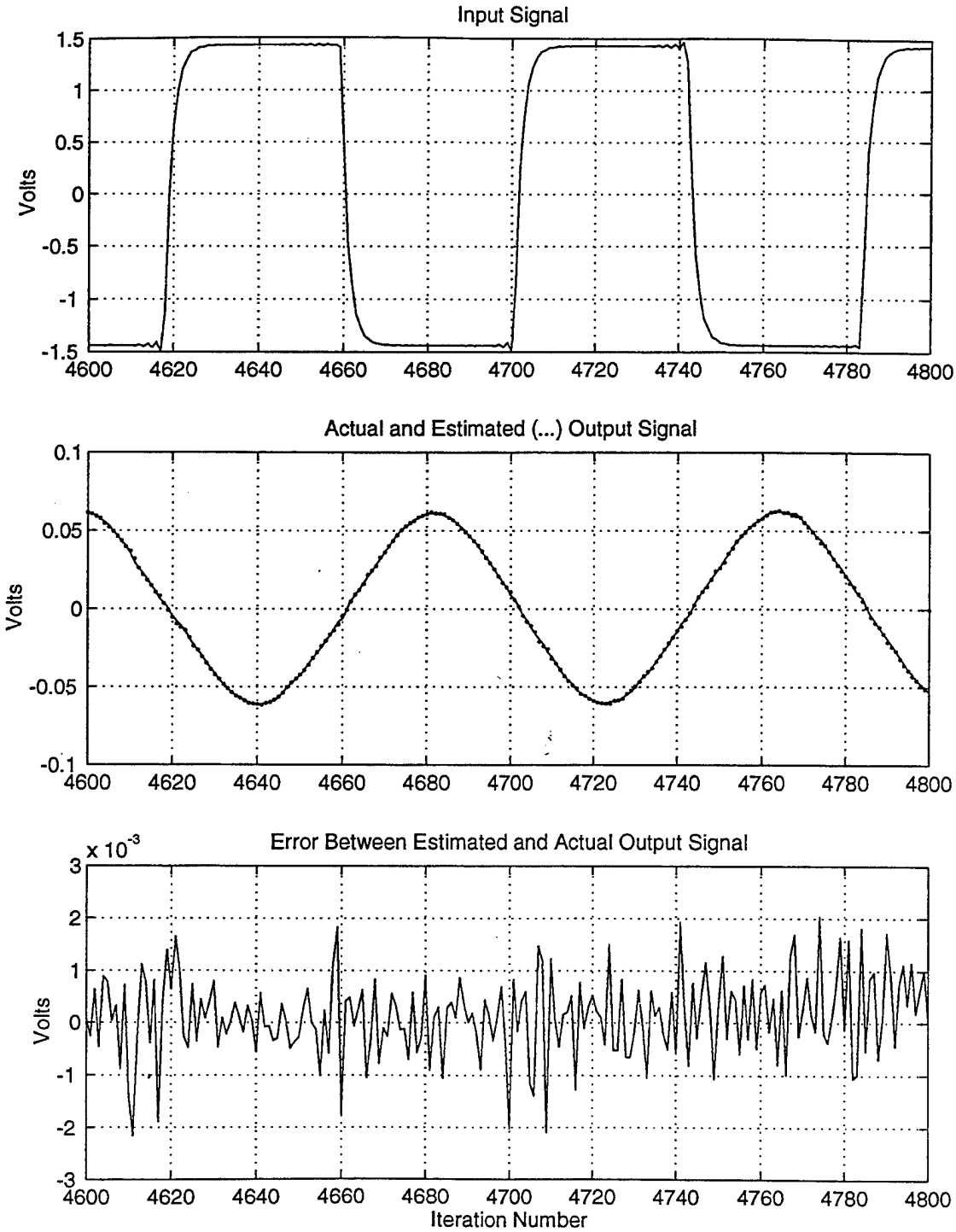

Figure 12e 580 Hz Sqare Flexural Waves in a Plastic Bar (L=156) Initial u=0.04

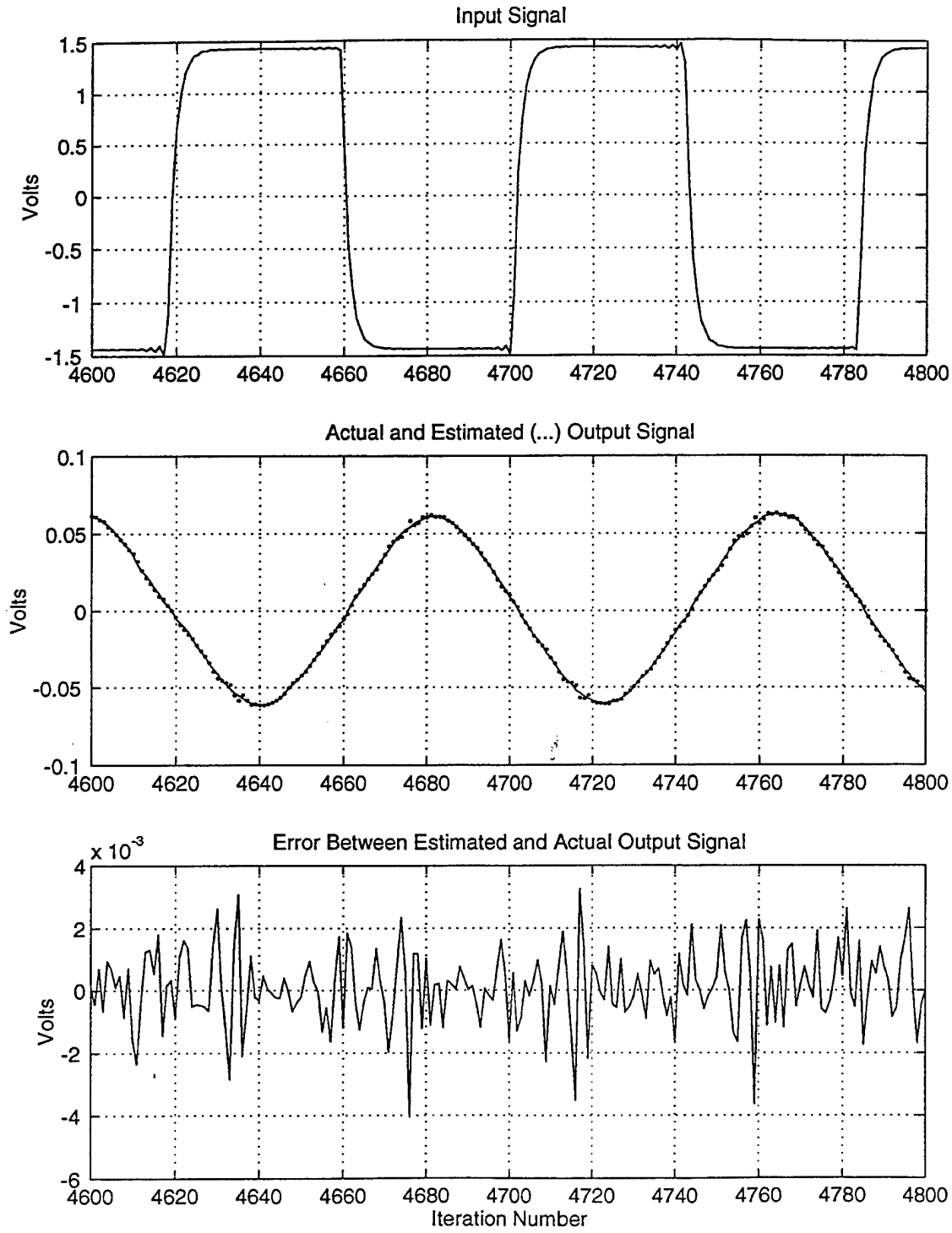

Figure 12f 580 Hz Sqare Flexural Waves in a Plastic Bar (L=166)
Initial u=0.04

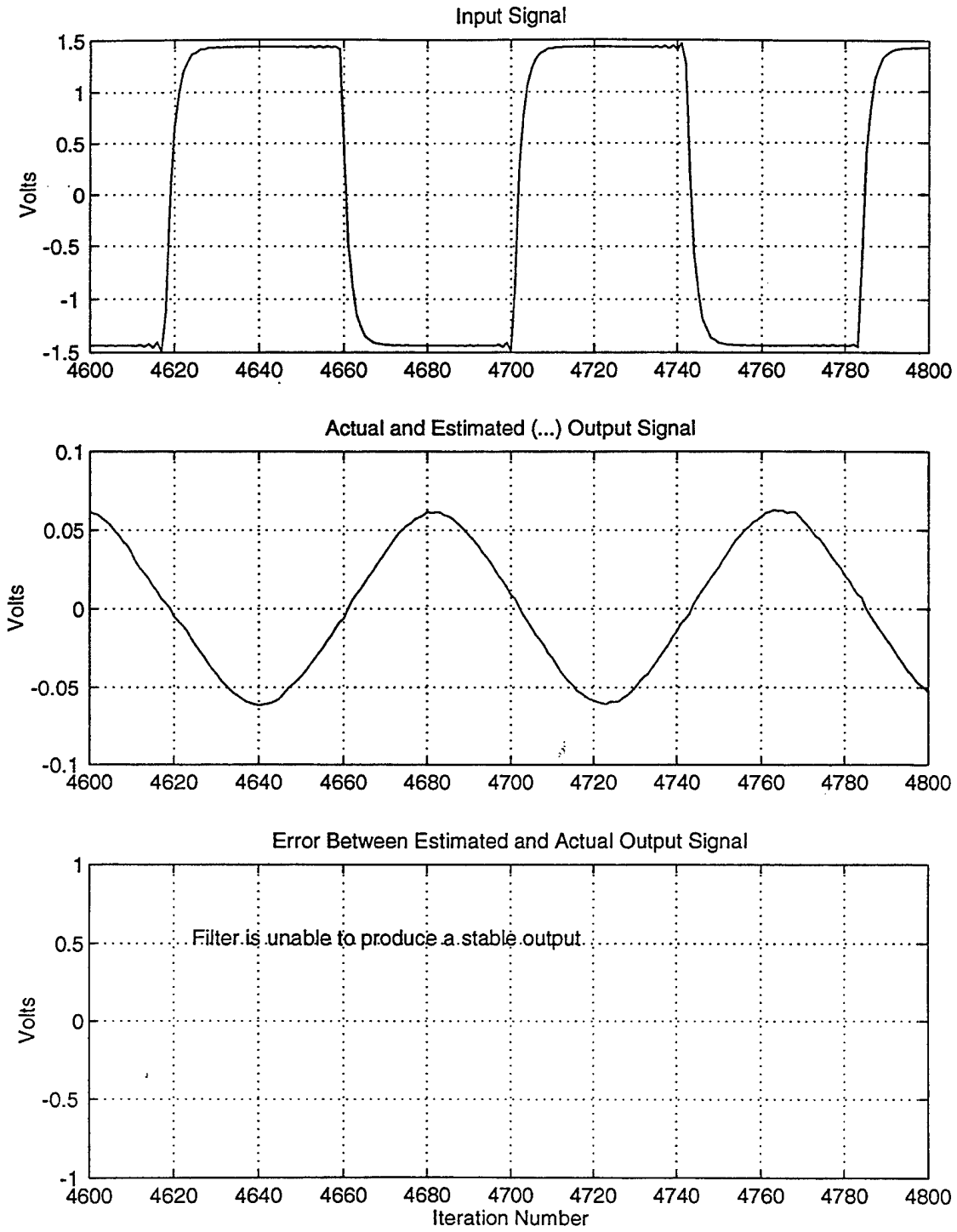

Figure 12g 580 Hz Sqare Flexural Waves in a Plastic Bar (L=167)
Initial u=0.04

converge on an optimal tap weight vector. Filter performance for the aluminum plate improved steadily as the Q was decreased by adding multiple layers of electrical tape and damping tape.

High Q systems such as the undamped bar and the ring (Q=1100) were not well modeled by the adaptive filter. Using longer tap weight vectors (as big as 2000) and increasing the number of iterations to as many as 16000 produced only a slight improvement in performance. However, filter performance could be improved somewhat by reducing the convergence parameter u by a factor of L as shown in Fig. 13 using data from the aluminum ring. An optimum value for L of 248 was used in this example by plotting error vs. tap weight vector length as was done in Fig. 11. Reducing u shortened the jumps down the performance surface that the filter took during each iteration. This method only improved performance in the case of high Q systems (Q>100). For low Q systems it drastically increased the error of the predicted output.

E. RECURSIVE VS. NONRECURSIVE ADAPTIVE FILTERS

In some cases recursive (IIR) filters outperformed nonrecursive (FIR) filters. Figures 14a and 14b show the performance of the adaptive filter (L=48) in predicting the output for a low Q (Q=8) system consisting of torsion waves, generated from white noise, traveling in a damped plastic bar. It is clear that the IIR filter performs better than the FIR filter. The improvement seen when using the IIR filter is due to the denominator term of the IIR filter which allows better modeling of the resonances present in the physical system. Similar results were obtained for the other nondispersive systems including those shown in Fig. 14c and 14d. These are the results of using torsion waves in a damped (Q=50) aluminum rod excited by broadband noise using a tap weight length of 128.

No improvement or only slight improvement was seen when using an IIR filter in dispersive systems as seen in Fig. 15a and 15b for flexural waves excited electromagnetically by broadband noise in a damped plastic bar (L=248). This is because in dispersive systems the traveling wave spreads out in time. The denominator term in the frequency response found in IIR systems is thus no longer as important

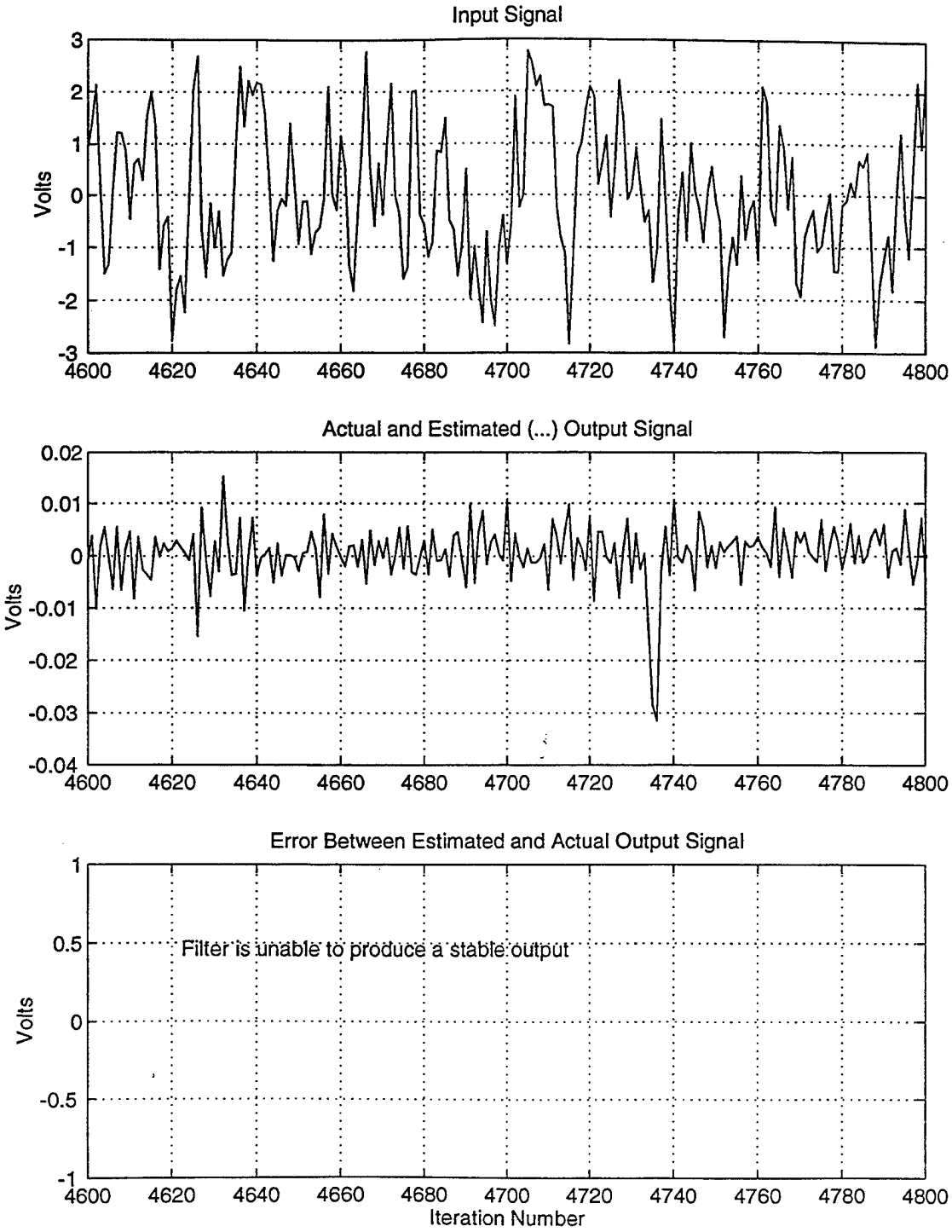

Figure 13a High Q System, Initial u=0.05
4800 Iterations, L=248

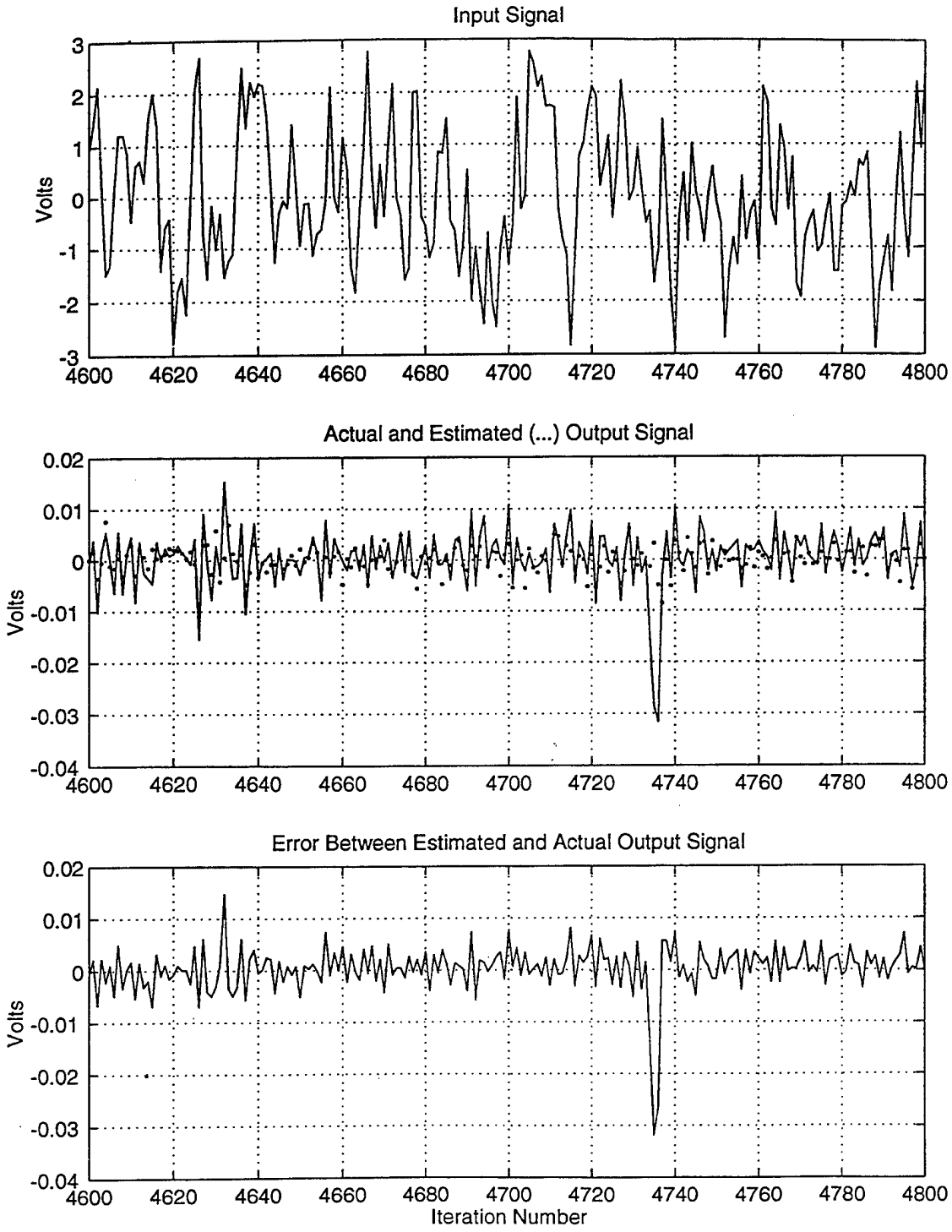

Figure 13b High Q System, Initial u=0.05/L
4800 Iterations, L=248

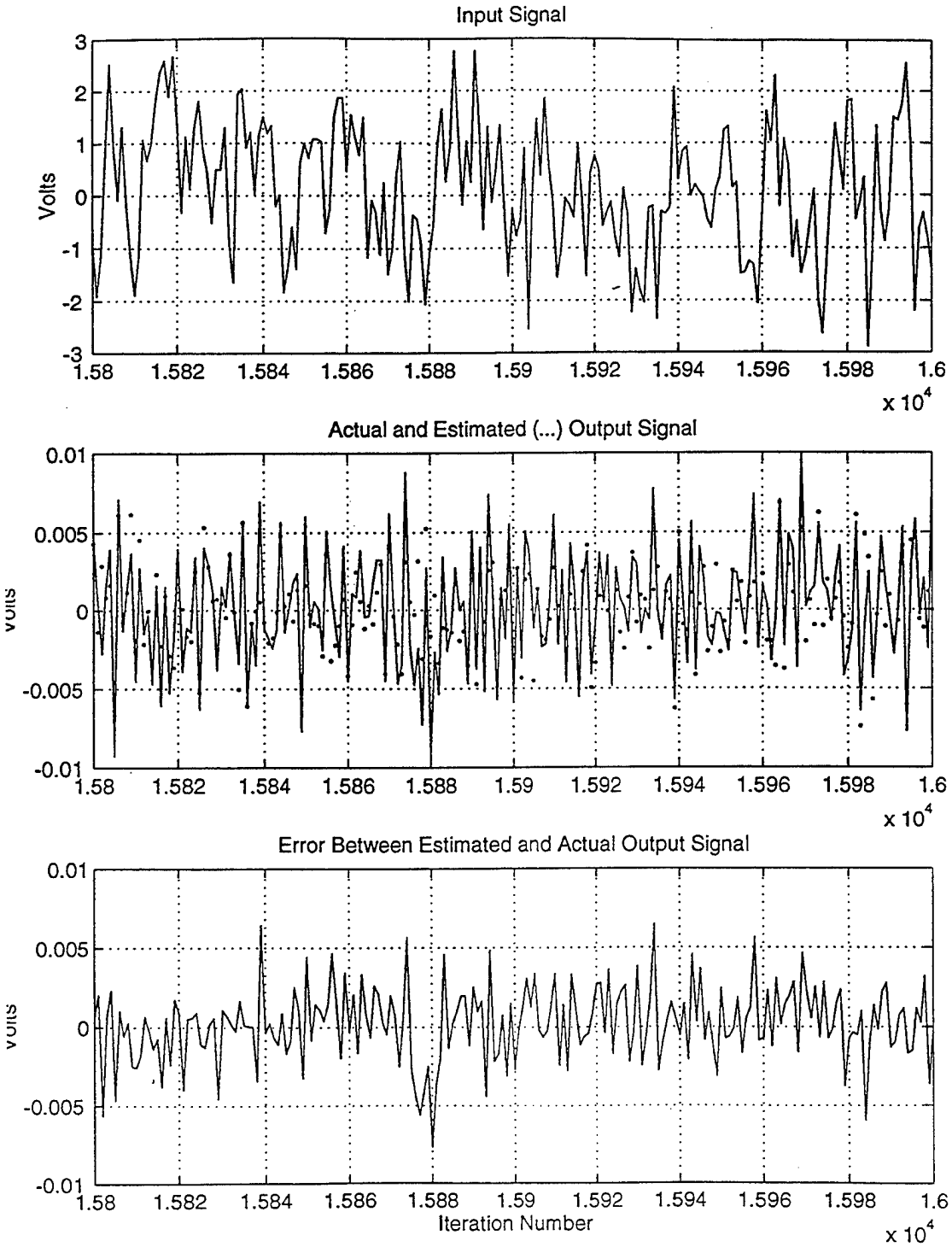

Figure 13c High Q System, Initial u=0.05/L
16000 Iterations, L=248

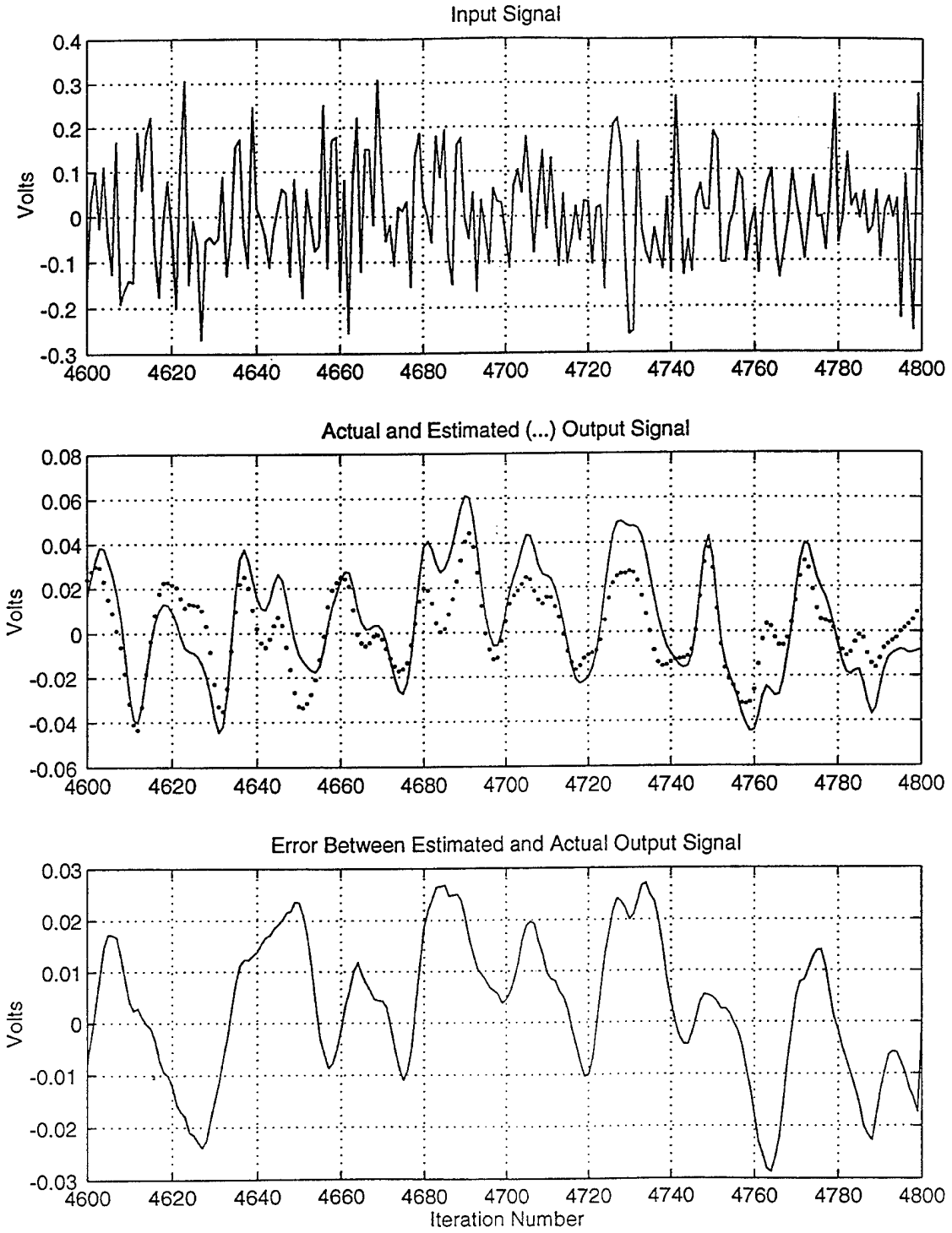

Figure 14a Results Using a FIR Filter on a Nondispersive System

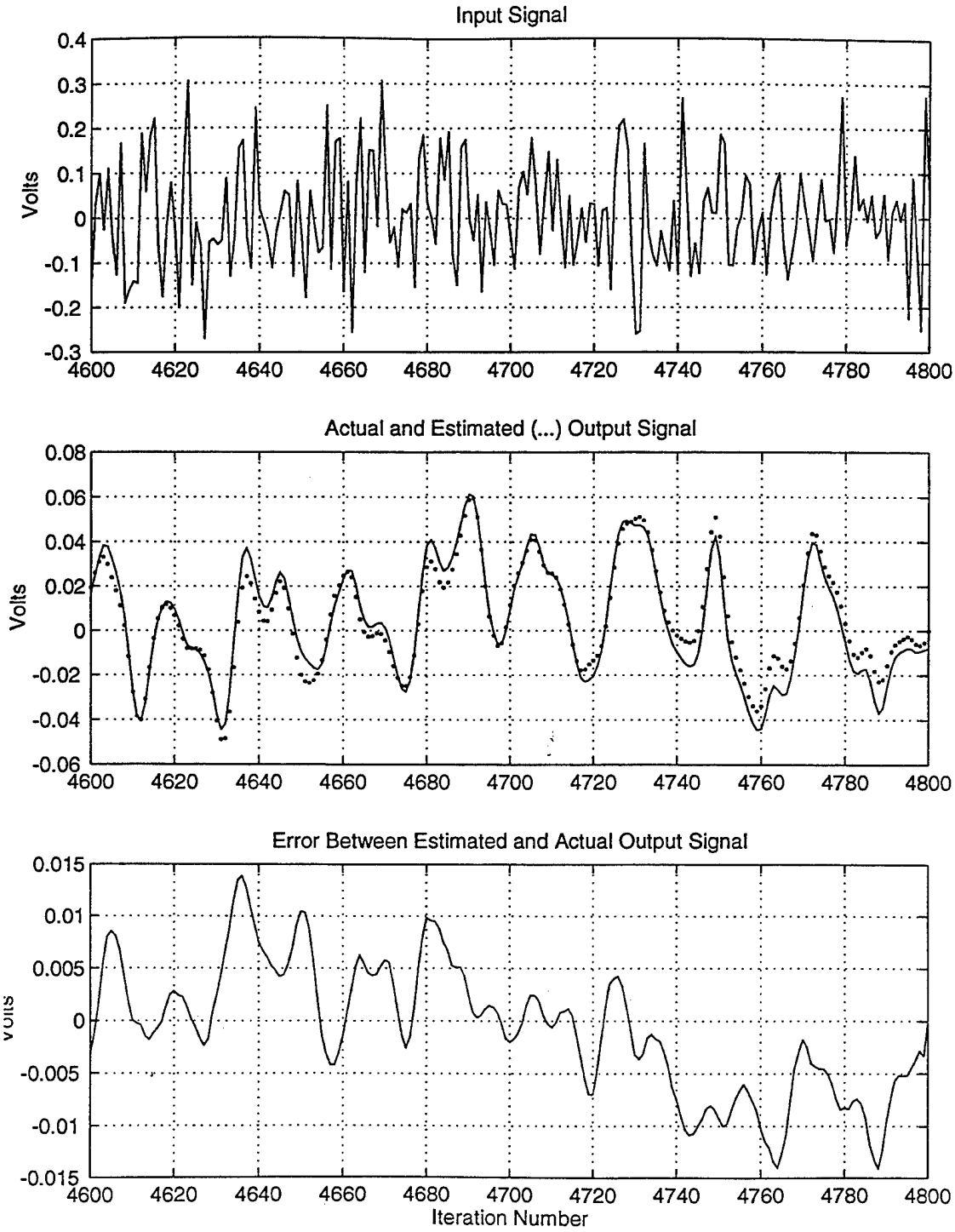

Figure 14b Results Using an IIR Filter on a Nondispersive System

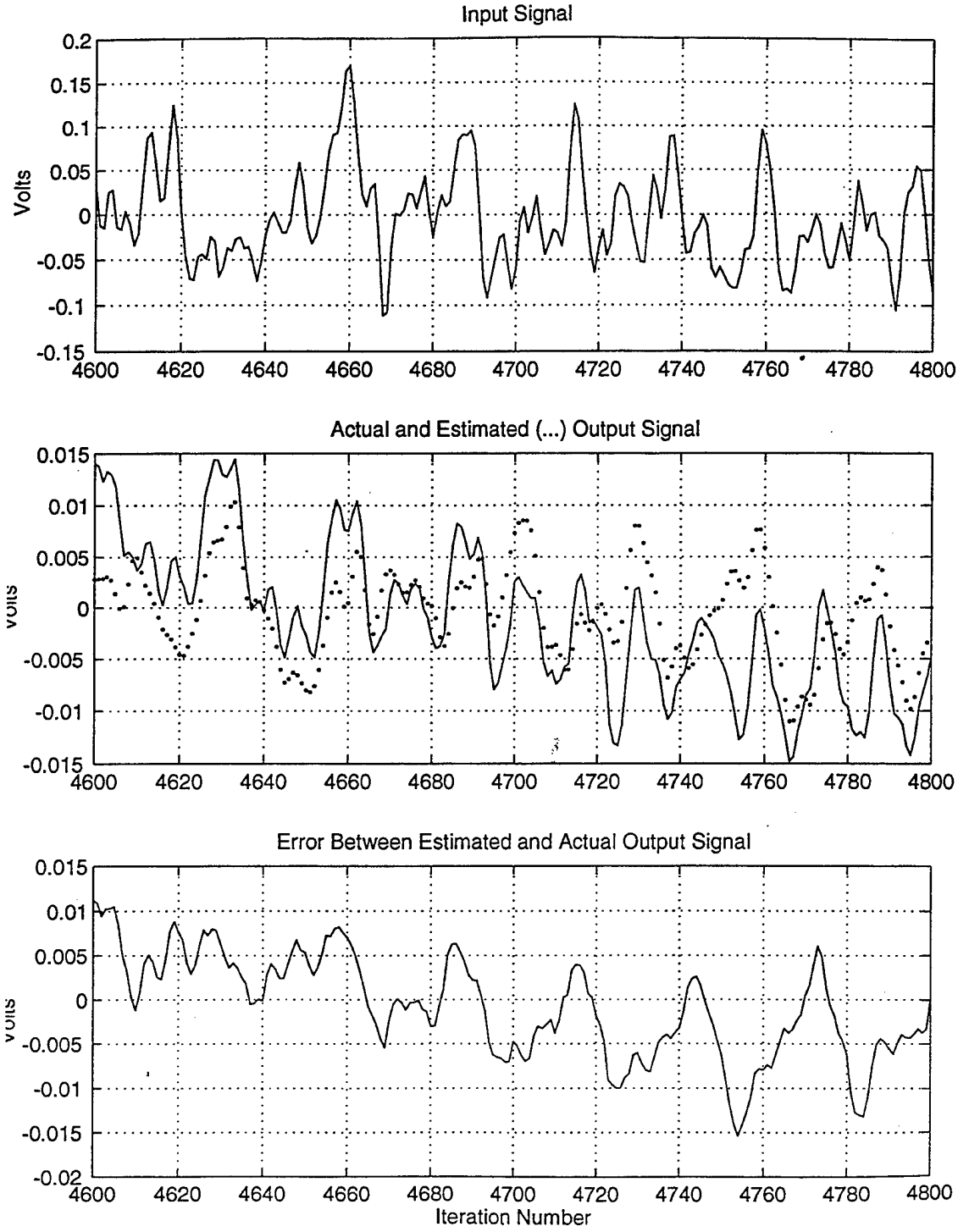

Figure 14c Results Using a FIR Filter on a Nondispersive System (Aluminum Bar)

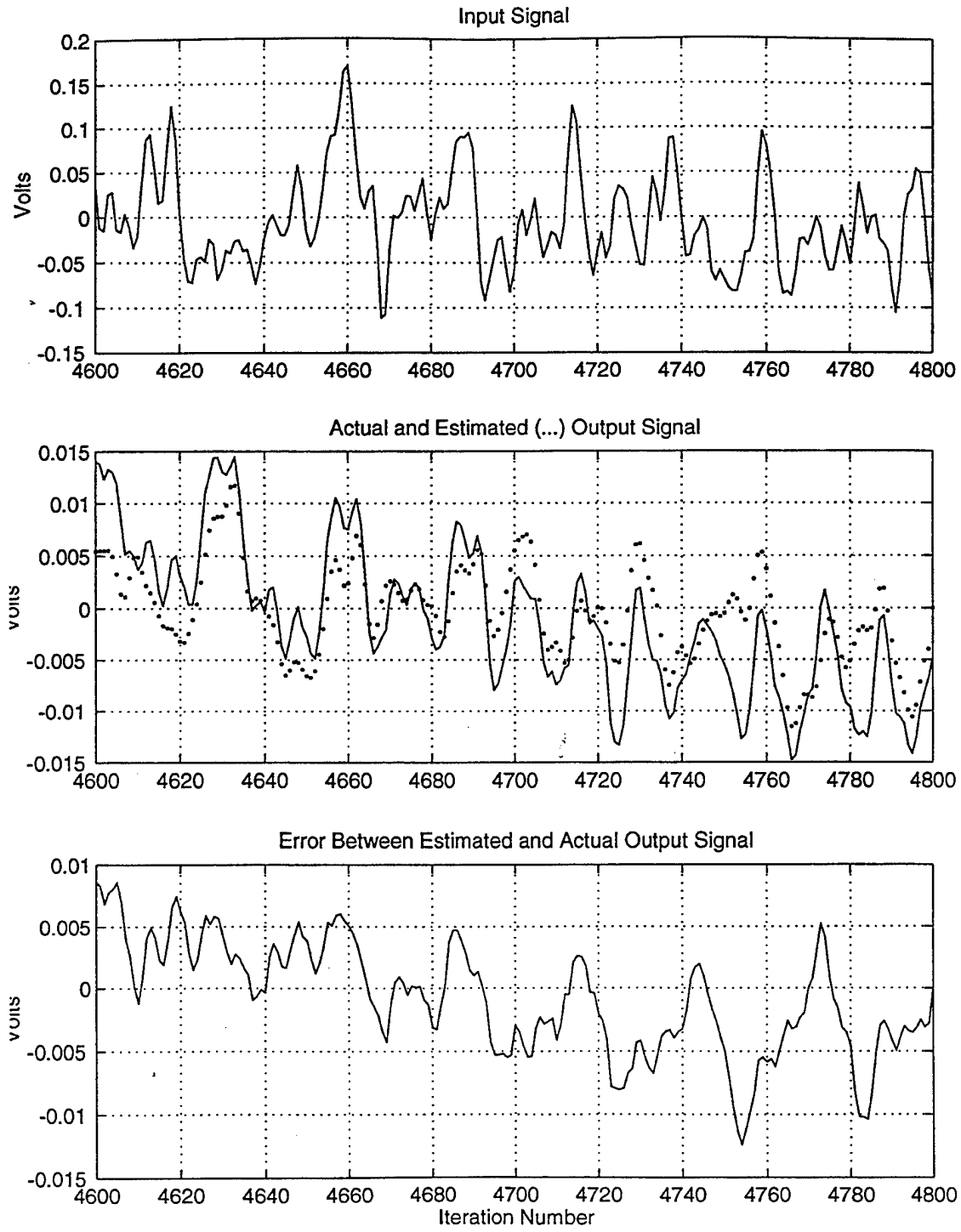

Figure 14d Results Using an IIR Filter on a Nondispersive System (Aluminum Bar)

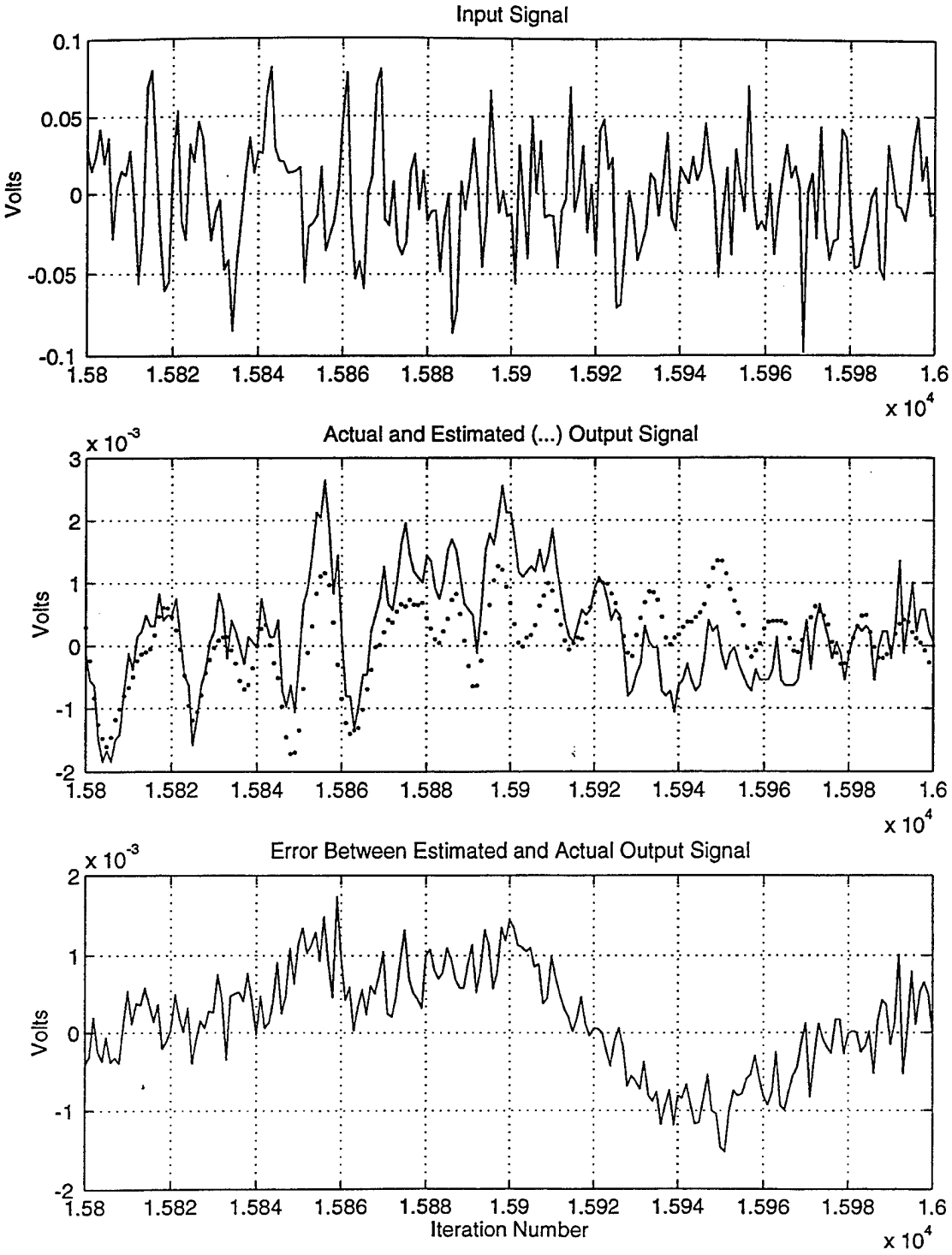

Figure 15a Results Using a FIR Filter on a Dispersive System

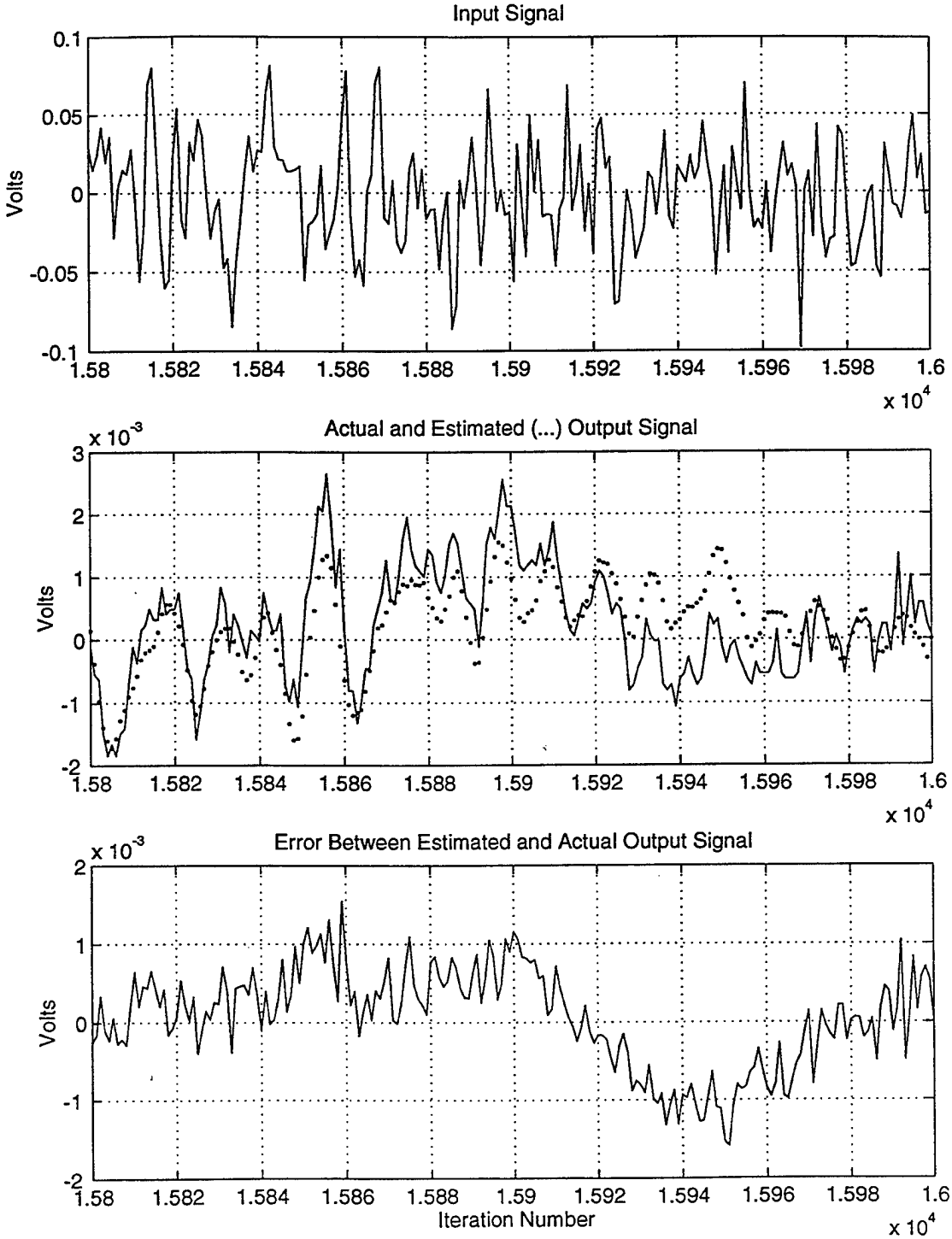

Figure 15b Results Using an IIR Filter on a Dispersive System

in determining the output from the input. Figures 15c and 15d show a similar result for flexural waves in a plastic bar generated by broadband noise driving a shaker table.

Stability is an important consideration in IIR filters. Instability is a result of the existence of poles in IIR filters which create a denominator term in the frequency response. Performance surfaces of IIR adaptive filters may have local minimums and may even be nonquadratic which could lead the tap weight vector to converge on a nonoptimal solution. However, no instability problems were seen when using an IIR filter on the simple mechanical systems investigated here. When instability was observed (when the tap weight vector failed to converge on a tap weight vector) both FIR and IIR filters were unable to converge on a tap weight vector for the experiment as discussed in section C of the results.

Both the FIR and the IIR filter performed better on the data from the shaker table experiment than on the data from waves generated electromagnetically. The shaker table generated "smoother" flexural waves than did the waves generated by electrodynamic transduction. The coils were attached to the bar by hand and could not be perfectly aligned to produce purely flexural waves. The electrodynamic transduction probably produced shear, longitudinal and torsional waves in addition to the flexural waves that were intended which made modeling by the adaptive filter difficult.

F. DISPERSIVE VS. NONDISPERSIVE PROPAGATION

In dispersive systems the adaptive filters generally behaved poorly. Performance was improved by using many more iterations than were used for nondispersive systems. While the nondispersive systems studied required several hundred iterations, the dispersive systems typically required at least 16000 iterations to produce a predicted output with a reasonable error. Figure 16 shows the result for flexural waves induced electromagnetically in a plastic bar after 4800 and 16000 iterations. Figure 17 shows a similar result for flexural waves produced by a shaker table. IIR filters were used for both figures.

An approach that might be more successful in performing system identification on dispersive systems is subband filtering. [Ref. 9] This would involve dividing the input signal into different frequency

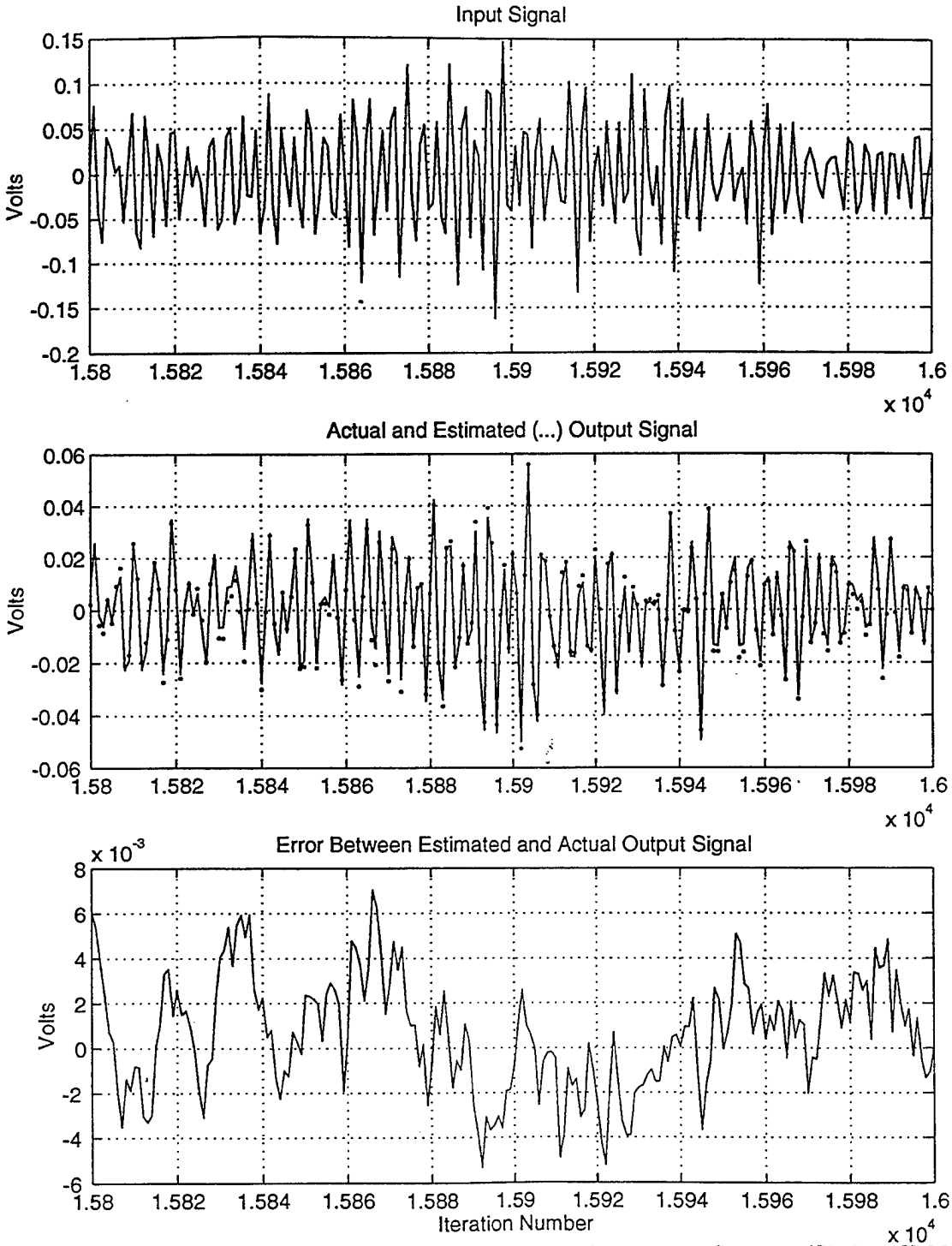

Figure 15c Results Using a FIR Filter on a Dispersive System (Shaker Table Data)

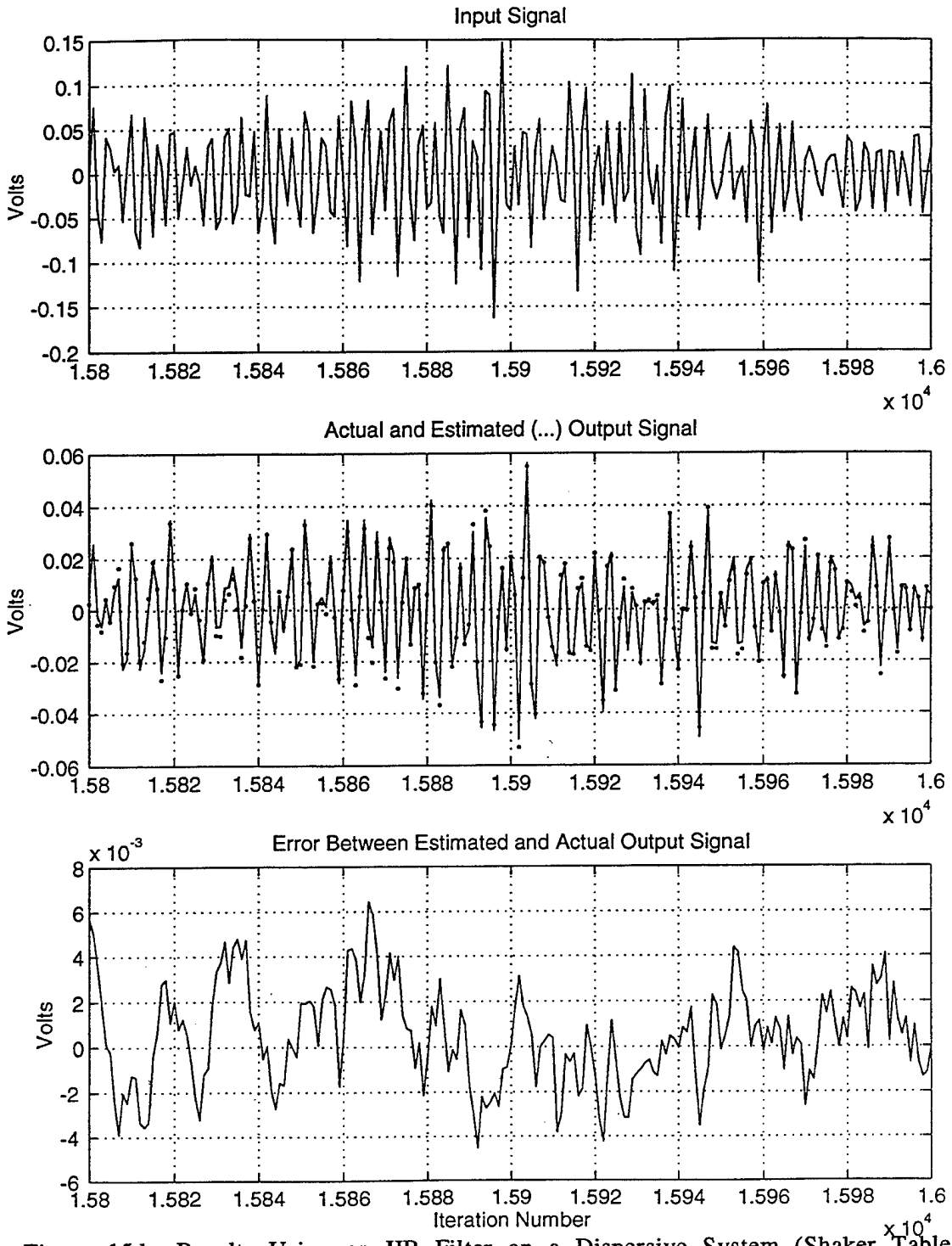

Figure 15d Results Using an IIR Filter on a Dispersive System (Shaker Table Data)

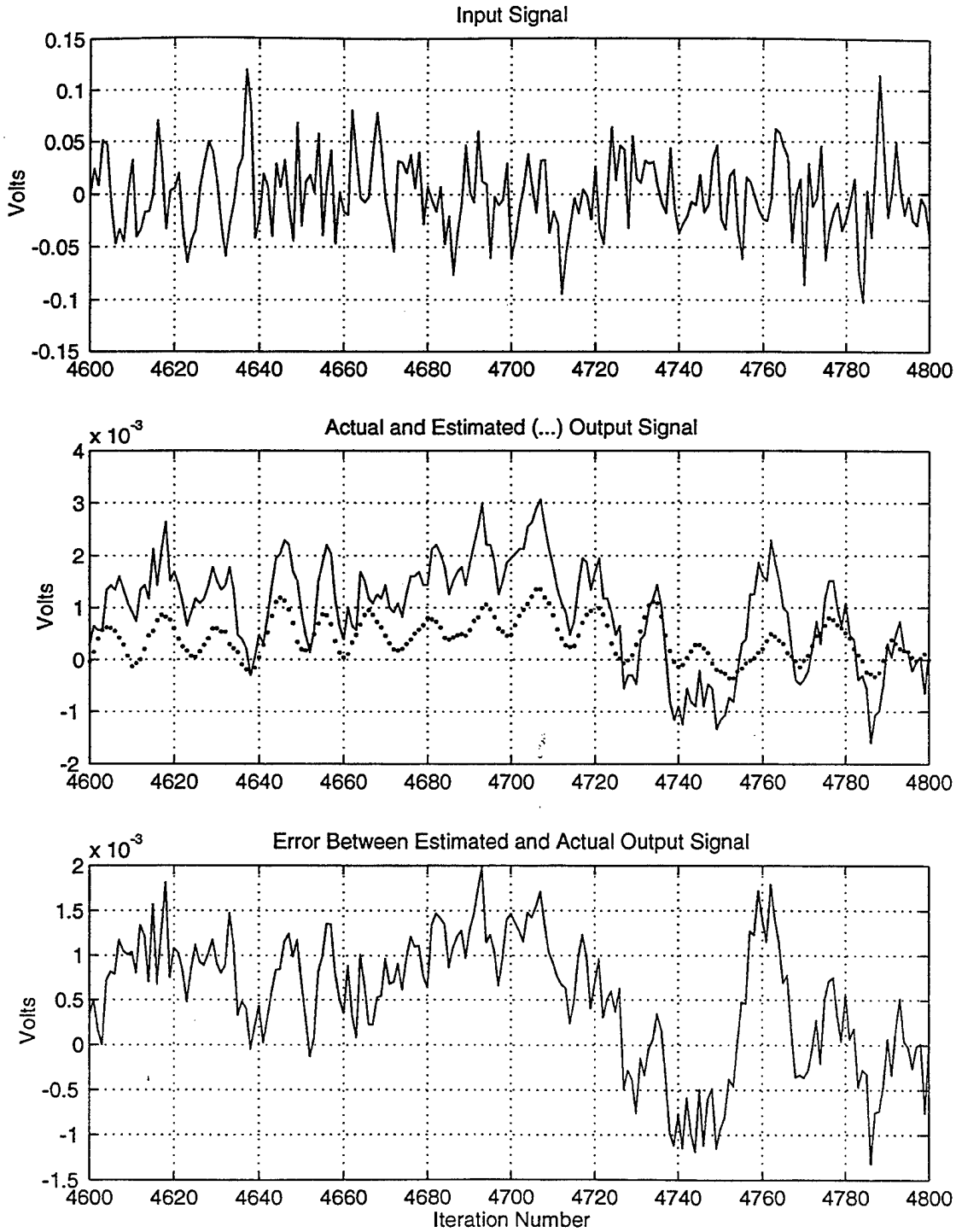

Figure 16a Results After 4800 Iterations for Flexural Waves (IIR Filter)

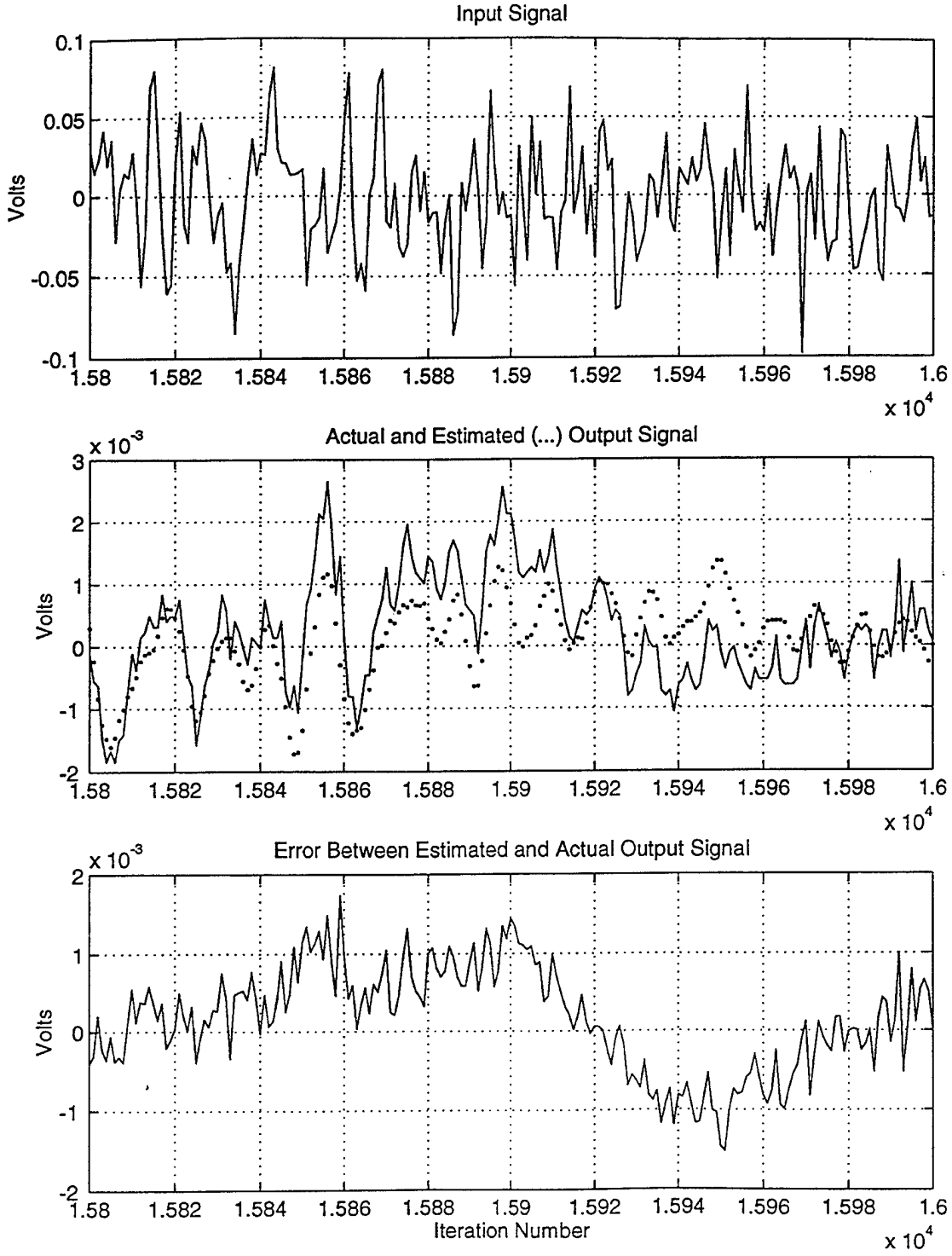

Figure 16b Results After 16000 Iterations for flexural Waves (IIR Filter)

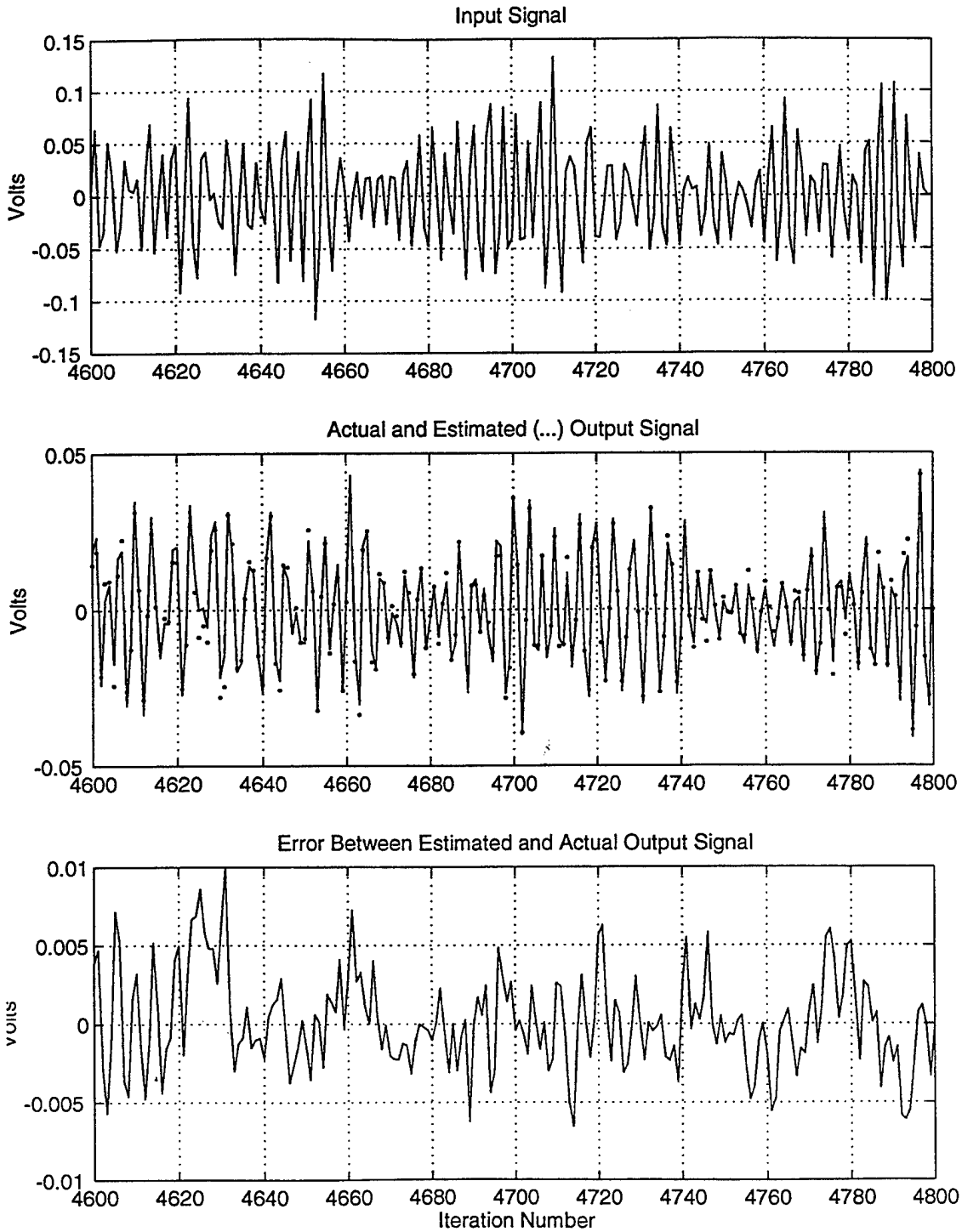

Figure 17a Results After 4800 Iterations for Flexural Waves - Shaker Table Data (IIR Filter)

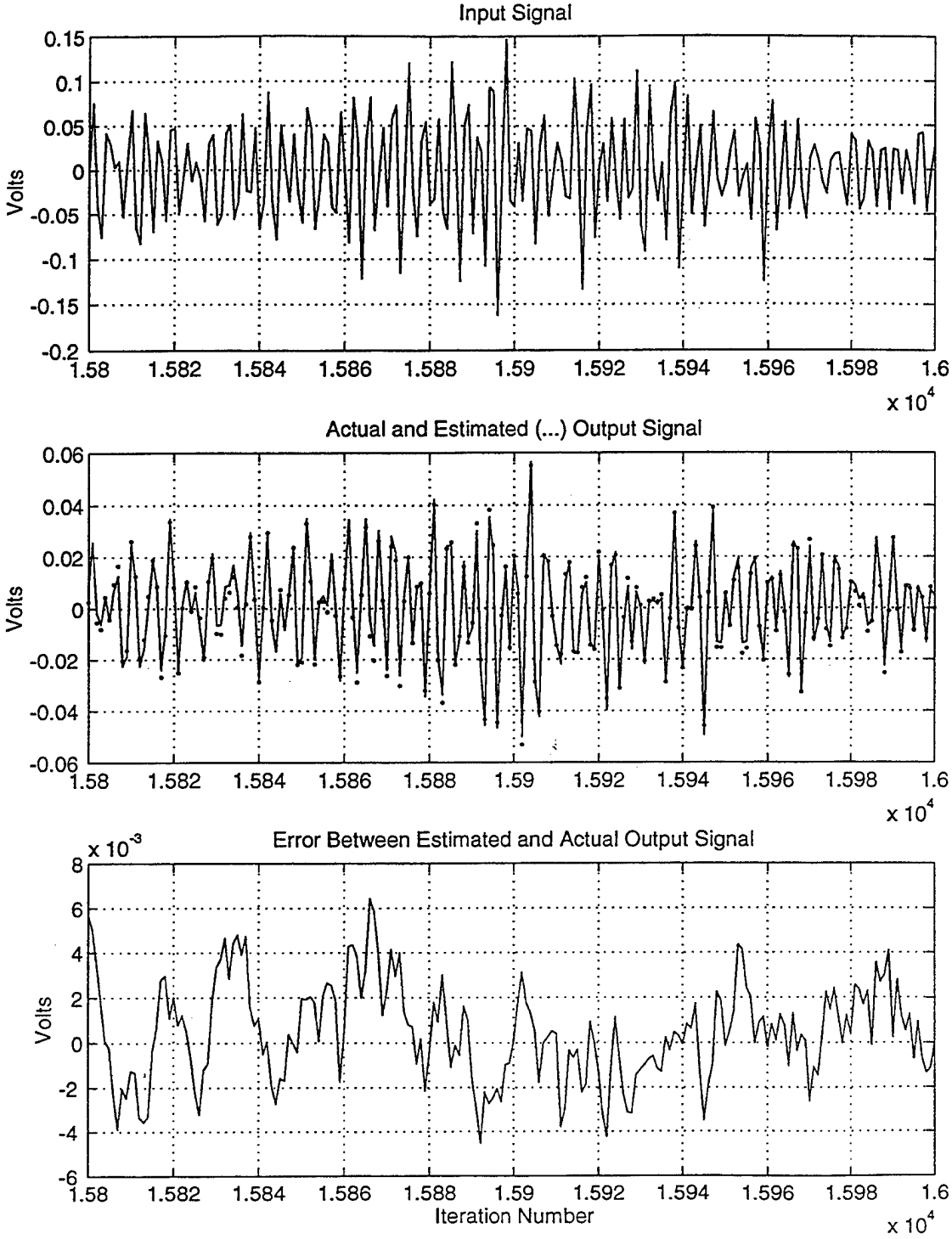

Figure 17b Results After 16000 Iterations for Flexural Waves-Shaker table Data (IIR Filter)

bands to be acted on by an individual adaptive filter for each band. A number of subband adaptive filter algorithms are available which also have the advantage of more closely tracking nonstationary systems.

G. COMPARISON WITH CROSS SPECTRAL DENSITY METHOD OF SYSTEM IDENTIFICATION

As discussed previously, Eq. 12 is commonly used to estimate the impulse response of single input, single output systems. Figure. 18a demonstrates that adaptive system identification produces a better estimate of the impulse response than does Eq. 12 for torsion waves in a damped plastic bar. The upper plot shows the output produced from an impulse response determined by an adaptive filter with a 128 element tap weight vector. Then, 128 element long samples were used to determine G_{xx} and G_{xy} and Eq. 12 was used to determine the frequency response. The inverse FFT of the frequency response was taken to determine the impulse response, h(t), which was used to produce the middle plot on Fig. 18a. The bottom plot on Fig. 18a compares the error associated with each method. Fig. 18b shows similar results for shaker table generated flexural waves in a plastic bar.

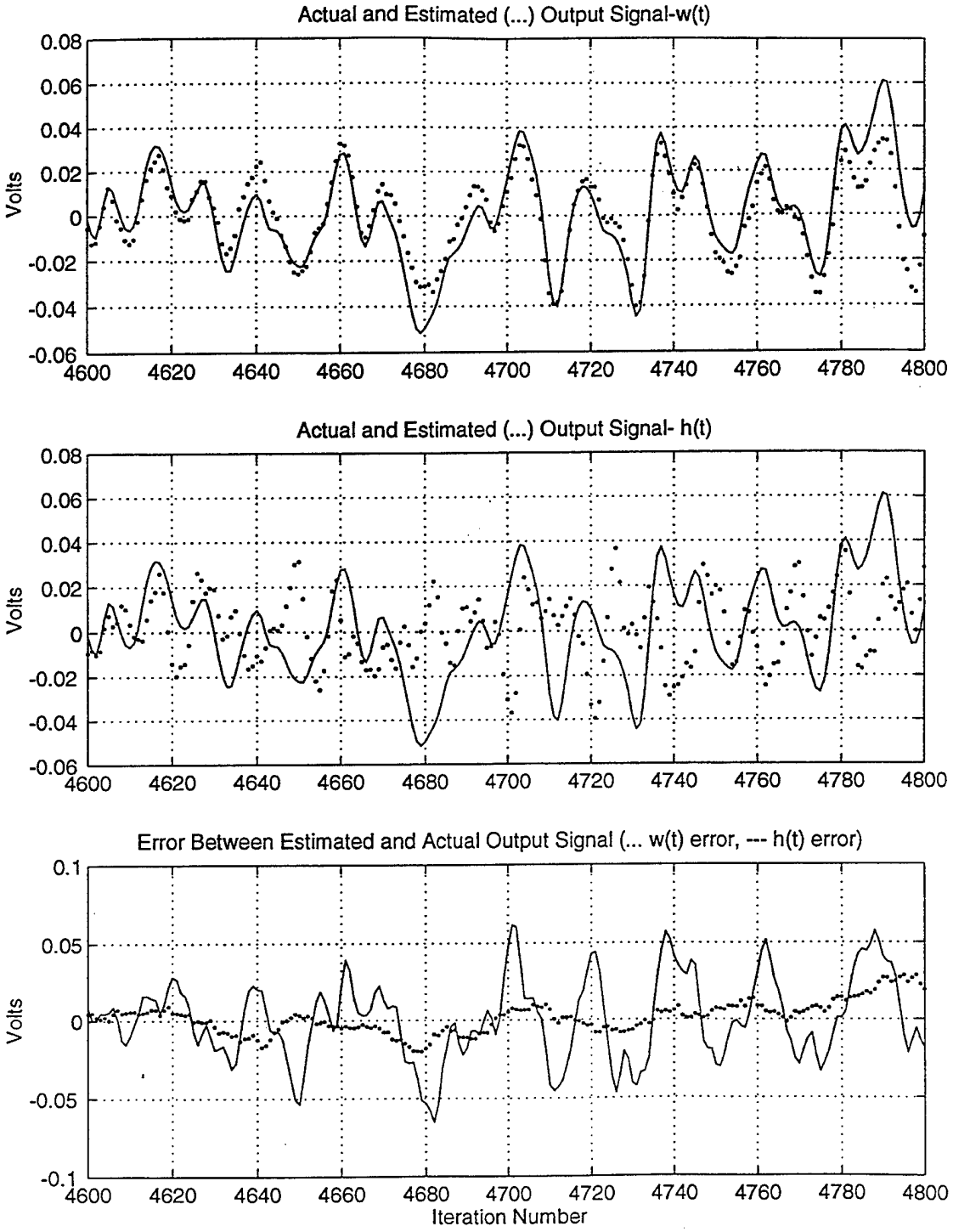

Figure 18a Comparison with Cross Spectral Density Method Damped Plastic Bar in Torsion Excited with Broadband Noise

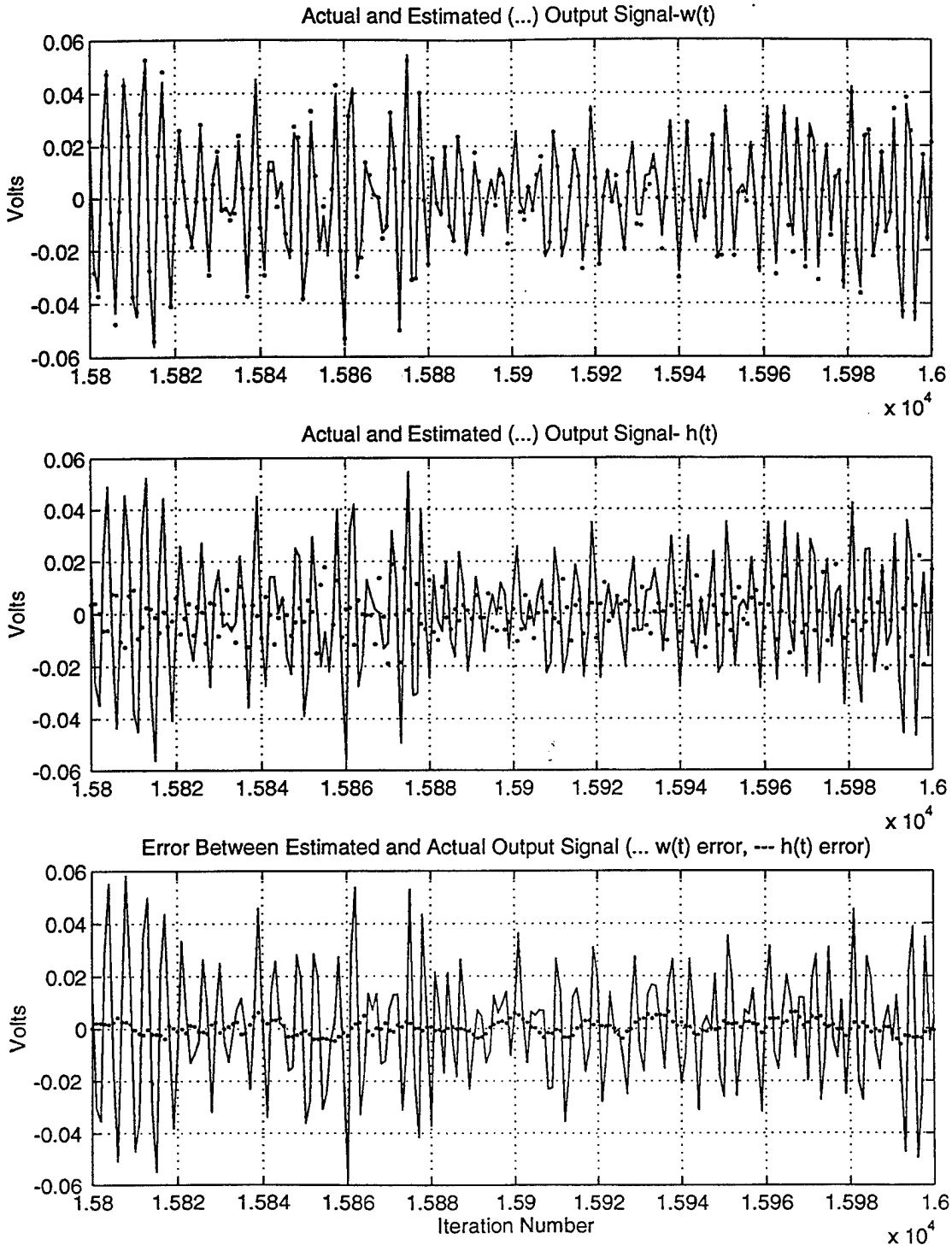

Figure 18b Comparison with Cross Spectral Density Method of System Identification Shaker Table Excited Flexural Waves in a Plastic Bar

V. CONCLUSION

The performance of adaptive filters used for system identification of mechanical systems depends greatly on the physical characteristics of that system. The propagation time, Q and dispersiveness of the mechanical system must be considered when modeling a mechanical system with an adaptive filter.

It is desirable to take into account the time necessary for vibration waves to propagate from the input of the system to the output so that the algorithm is not utilizing data from mismatched times. This was shown to be quite simple in the case of a torsion wave traveling down a plastic bar. However, in complex, multipath systems determining this propagation time would be much more difficult. In the multipath aluminum plate and ring experiments the performance of the adaptive filter was degraded by delaying the input to account for propagation time. More research is required to see if the this concept is applicable to a very complex system such as a submarine.

The high Q systems investigated were not well modeled by the adaptive algorithm. The adaptive filters required very small values of the step size parameter u to be effective. The dispersive systems studied required many more iterations than nondispersive systems (by a factor of about 20) to determine a good estimate of the mechanical impulse response. Again, more research is required to determine what role these factors would play in a complex mechanical structure.

The adaptive filter method of system identification was compared to the more conventional method of utilizing the cross spectral and autospectral densities of the input and output signals. For the simple mechanical systems studied here the adaptive filter performed better.

It is hoped that the benefits of considering the physical parameters of a system when performing system identification with adaptive filters will also prove valuable to other, more advanced methods of system identification.

APPENDIX. DERIVATION OF THE CHARACTERISTIC DISPERSION TIME

In dispersive systems a pulse will spread out in time because its different Fourier components travel at different speeds. In order to quantify the effect of the dispersion in "stretching" the pulse over time, a "characteristic dispersion time" was defined. This constant is useful in evaluating the convergence performance of adaptive filters when modeling dispersive systems. The derivation is begun by stating that the angular frequency of the second flexural mode ω_2 is related to ω_1 , the angular frequency of the first flexural mode by:

$$\omega_2 = 2\omega_1(1+\varepsilon_2), \tag{A1}$$

where ε_2 is a factor to account for the anharmonic nature of dispersive waves. Multiplying both sides by time results in:

$$\omega_2 t = 2\omega_1(1+\varepsilon_2)t, \tag{A2}$$

which can be reduced to

$$\phi_2 - 2\phi_1 = 2\phi_1\varepsilon_2. \tag{A3}$$

An arbitrary criteria was selected to describe the point at which the two modes were so out of phase that the pulse was appreciably spread out in time. The time for this to occur will be called the characteristic dispersion time. This criteria was selected to be:

$$\omega_2 t - 2\omega_1 t = \pi/2. \tag{A4}$$

Solving for time gives:

$$t = \pi / 2(\omega_2 - 2\omega_1).$$

Since the angular frequency is equal to 2π times the frequency in Hertz,

$$t = \pi / 2(2\pi f_2 - 4\pi f_1)$$

or

$$t = 1 / (4f_2 - 8f_1). \tag{A5}$$

Computing the frequencies of the first two modes of flexural waves in the plastic bar using Eq. 10 results in $f_1 = 81.7$ Hz and $f_2 = 225.3$ Hz. From Eq. A5 this results in a dispersion time constant of 4.0 ms.

The characteristic dispersion time for the n^{th} mode to shift its phase by $\pi/2$ (a quarter cycle) with respect to the nondispersive case (n times the fundamental frequency) can be computed using:

$$t = 1 / (4f_n - 4nf_1). \tag{A6}$$

A characteristic dispersion time was also calculated for the case of torsion wave propagation. Theoretically there should not be any dispersion for torsion waves but due to imperfections in the transducers and in the bar itself some dispersion will occur in all practical systems. Additionally, the derivation of Eq. 9 assumes that the edge of the bar is rigid and cannot move which is not actually the case. The first two torsional resonant frequencies of the damped plastic bar were determined experimentally to be 1.112 kHz and 2.15 kHz. Equation A6 was used to give a value of 3.4 seconds for the characteristic dispersion time. The time is much longer than for the flexural wave case because the torsion waves are much less dispersive.

LIST OF REFERENCES

1. Widrow, B. and Stearns, S.D., *Adaptive Signal Processing*, pp. 1-11, Prentice-Hall, Englewood Cliffs , NJ, 1985.

2. Widrow et al., "Adaptive Noise Cancelling: Principles and Applications," *Proceedings of the IEEE.*,vol. 63, no. 12, pp.1692-1694 (1975).

3. Widrow, B. and Stearns, S.D, pp. 19-21, 99-106.

4. Widrow, B. and Stearns, S.D, pp. 110-114.

5. Coppens, A.B., Frey, A.R., Kinsler, L.E., Sanders, J.V., *Fundamentals of Acoustics,* pp. 57-75, John Wiley & Sons, New York, 1982.

6. Garrett, S., "Resonant Acoustic Determination of Elastic Moduli, " *Journal of the Acoustical Society of America.*,vol. 88, no. 1, pp.210-221 (1990).

7. Bendat, J.S., and Pearsol, A.G., *Engineering Applications of Correlation and Spectral Analysis*, pp. 97-100, John Wiley & Sons, New York, 1980.

8. Kirk, D.E. and Strum, R.D., *First Principles of Discrete Systems and Digital Signal Processing*, Addison-Wesley Publishing Company, 1989.

9. Goubran, R.A., and Wallace, R.B., "Noise Cancellation Using Parallel Adaptive Filters," *IEEE Transactions on Circuits and Systems* , vol. 39, no. 4, pp. 239-243 (1993).

10. Byung-Eul Jun and Dong-Jo Park, "Novel Steepest Decent Adaptive Filter Derived From New Performance Function with Additional Exponential Term," *Signal Processing* 36, 1994, pp.189-199.

11. LabVIEW Version 3.0, National Instruments Inc., Austin, Tx. (Using the NBA-2150F Analog to Digital Converter Board).

12. Matlab for the Macintosh Version 4.2c, The Mathworks, Natick, Ma.

13. Coppens, A.B., Frey, A.R., Kinsler, L.E., Sanders, J.V, pp. 11.

14. Coppens, A.B., Frey, A.R., Kinsler, L.E., Sanders, J.V, pp. 16.

INITIAL DISTRIBUTION LIST

1. Defense Technical Information Center 2
   8725 John J. Kingman Road, Ste 0944
   Ft. Belvoir, Virginia 22060-6218

2. Dudley Knox Library 2
   Naval Postgraduate School
   411 Dyer Rd.
   Monterey, California 93943-5101

3. Professor Robert Keolian PH/KN 4
   Department of Physics
   Naval Postgraduate School
   Monterey, California 93943-5103

4. Professor Roberto Cristi EC/CX 2
   Department of Electrical and Computer Engineering
   Naval Postgraduate School
   Monterey, California 93943-5103

5. Lt Michael Dargel 1
   8 Willow Lane
   East Lyme, Ct 06333